



January 2017

# Effect Of Bio-Binders On Binder And Mix Properties With High Rap Content

Rajib Chandra Saha

Follow this and additional works at: <https://commons.und.edu/theses>

---

## Recommended Citation

Saha, Rajib Chandra, "Effect Of Bio-Binders On Binder And Mix Properties With High Rap Content" (2017). *Theses and Dissertations*. 2331.

<https://commons.und.edu/theses/2331>

This Thesis is brought to you for free and open access by the Theses, Dissertations, and Senior Projects at UND Scholarly Commons. It has been accepted for inclusion in Theses and Dissertations by an authorized administrator of UND Scholarly Commons. For more information, please contact [zeinebyousif@library.und.edu](mailto:zeinebyousif@library.und.edu).

EFFECT OF BIO-BINDERS ON BINDER AND MIX PROPERTIES WITH HIGH RAP  
CONTENT

by

Rajib Chandra Saha  
Bachelor of Science in Civil Engineering, Bangladesh University of Engineering and  
Technology, 2009  
Master of Development Studies, University of Dhaka, 2013

A Thesis

Submitted to the Graduate Faculty

of the

University of North Dakota

In partial fulfillment of the requirements

for the degree of

Master of Science

Grand Forks, North Dakota

August  
2017

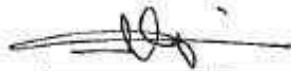
Copyright 2017 Rajib Chandra Saha

This thesis, submitted by Rajib Chandra Saha in partial fulfillment of the requirements for the Degree of Master of Science from the University of North Dakota, has been read by the Faculty Advisory Committee under whom the work has been done and is hereby approved.



6/23/2017

Dr. Daba Gedafa, P.E., Chairperson

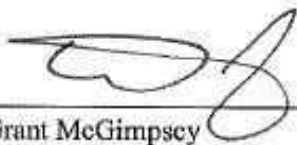


Dr. Nabil Suleiman



Mr. Bruce Dockter, P.E.

This thesis is being submitted by the appointed advisory committee as having met all of the requirements of the School of Graduate Studies at the University of North Dakota and is hereby approved.



Grant McGimpsey  
Dean of the School of Graduate Studies

June 30, 2017

Date

## PERMISSION

Title           Effect of Bio-Binders on Binder and Mix Properties with High RAP  
                  Content

Department   Civil Engineering

Degree        Master of Science

In presenting this thesis in partial fulfillment of the requirements for a graduate degree from the University of North Dakota, I agree that the Library of this University shall make it freely available for inspection. I further agree that permission for extensive copying for scholarly purposes may be granted by the professor who supervised my thesis work or, in his absence, by the Chairperson of the department or the dean of the School of Graduate Studies. It is understood that any copying or publication or other use of this thesis or part thereof for financial gain shall not be allowed without my written permission. It is also understood that due recognition shall be given to me and to the University of North Dakota in any scholarly use which may be made of any material in my thesis.

Rajib Chandra Saha

6/23/2017

## TABLE OF CONTENTS

<b>TABLE OF CONTENTS</b> .....	<b>v</b>
<b>LIST OF FIGURES</b> .....	<b>viii</b>
<b>LIST OF TABLES</b> .....	<b>xi</b>
<b>ACKNOWLEDGEMENTS</b> .....	<b>xii</b>
<b>ABSTRACT</b> .....	<b>xiii</b>
<b>CHAPTER</b>	
<b>I. INTRODUCTION</b> .....	<b>1</b>
1.1 General .....	1
1.2 Reclaimed Asphalt Pavement (RAP) and Sustainability .....	1
1.3 Bio-binder.....	3
1.4 Performance Properties of Asphalt Pavement.....	4
1.5 Problem Statement .....	4
1.6 Objectives.....	5
1.7 Methodology .....	5
1.8 Organization of Thesis .....	5
<b>II. LITERATURE REVIEW</b> .....	<b>7</b>
2.1 General .....	7
2.2 High percentage of RAP usages in HMA .....	8
2.3 Asphalt Chemistry.....	10
2.4 Bio-Oil.....	11
2.4.1 Waste Cooking Oil (WCO) .....	11
2.4.2 Soy-Oil.....	12
2.5 Binder Rheology .....	13
2.5.1 Medium and High-Temperature Rheology.....	14

2.5.2 Low-Temperature Rheology.....	14
2.6 Cracking potential of HMA and Tests .....	15
2.7 Intermediate Temperature Cracking and SCB Test .....	16
2.8 Asphalt Pavement Low-Temperature Cracking and DCT Test .....	18
2.9 Asphalt Pavement Rutting.....	18
2.10 Bio-Oil modified binder and mix with High RAP Binder .....	19
<b>III. METHODOLOGY.....</b>	<b>21</b>
3.1 Experimental Plan .....	21
3.2 Materials Selection.....	23
3.3 RAP Binder Extraction and Selection of Solvent .....	24
3.4 Dynamic Shear Rheometer (DSR) Test .....	28
3.5 Rolling Thin Film Oven (RTFO) Test .....	32
3.6 Pressurized Aging Vessel (PAV) Test .....	33
3.7 Mix Design.....	34
3.8 HMA compaction.....	36
3.9 Rutting Resistance Test by APA.....	37
3.10 Low-temperature Cracking Resistance Test by DCT .....	38
3.11 Fatigue Cracking Test by SCB.....	40
3.12 Data Analysis .....	41
<b>IV. RESULTS AND DISCUSSIONS .....</b>	<b>43</b>
4.0 General .....	43
4.1 Effect of Bio-binders on Binder Rheology .....	43
4.1.1 Rutting Resistance .....	44
4.1.2 Fatigue Resistance .....	49
4.1.3 Low-Temperature Cracking Resistance .....	53
4.2 Effect of Bio-binders on HMA Mix.....	60
4.2.1 Rutting Resistance .....	60
4.2.2 Fatigue Cracking Resistance .....	65
4.2.3 Low-Temperature Cracking Resistance .....	70
<b>V. CONCLUSIONS AND RECOMMENDATIONS.....</b>	<b>73</b>
5.0 General .....	73

5.1 Rutting Resistance.....	73
5.2 Fatigue Resistance.....	74
5.3 Low-Temperature Cracking Resistance .....	75
5.4 Limitations .....	75
5.5 Future Works.....	75
<b>REFERENCES.....</b>	<b>77</b>
<b>APPENDICES.....</b>	<b>83</b>



## LIST OF FIGURES

Figure 1: Energy savings and CO2 reduction at different RAP content levels (Lee et al., 2012). .....	2
Figure 2: Typical Load-Displacement curve obtained from SCB test (Ozer et al., 2016). .....	17
Figure 3: Flow Chart of Phase I test plan. ....	22
Figure 4: Flow Chart of Phase II test plan. ....	23
Figure 5: Extraction Bowl Unit (ASTM, 2011). ....	26
Figure 6: Fractional Distillation Unit by Abson Method (ASTM, 2003). ....	27
Figure 7: DSR test setup. ....	28
Figure 8: Applied Shear Stress and Resulting Shear Strain on Asphalt (Pavement Interactive, 2016). ....	29
Figure 9: Complex Shear Modulus (Pavement Interactive, 2016). ....	30
Figure 10: RTFO oven. ....	32
Figure 11: PAV vessel. ....	33
Figure 11: Superpave Gyrotory Compactor. ....	36
Figure12: APA machine test chamber. ....	37
Figure 13: Dimension of DCT Specimen (ASTM 2013). ....	39
Figure 14: DCT test setup. ....	40
Figure 15: SCB test specimen Geometry (AASHTO, 2016). ....	41
Figure 16: SCB test setup. ....	41
Figure 17: Unaged binders in different combination of bio-binder and RAP binder @ 58°C with 100% RAP binder. ....	45

Figure 18: Unaged binders in different combination of bio-binder and RAP binder @ 58°C without 100% RAP binder. ....	45
Figure 19: Unaged binders in different combination of bio-binder and RAP binder @ 64°C with 100% RAP binder. ....	46
Figure 20: Unaged binders in different combination of bio-binder and RAP binder @ 64°C without 100% RAP binder. ....	46
Figure 21: RTFO aged binders in different combination of bio-binder and RAP binder @ 58°C with 100% RAP binder. ....	48
Figure 22: RTFO aged binders in different combination of bio-binder and RAP binder excluding 100% RAP binder @ 58°C without 100% RAP binder. ....	48
Figure 23: RTFO aged binders of different combination of bio-binder and RAP binder @ 64°C with 100% RAP binder. ....	49
Figure 24: RTFO aged binders of different combination of bio-binder and RAP binder excluding 100% RAP binder @ 64°C without 100% RAP binder. ....	49
Figure 25: PAV aged binders in different combination of bio-binder and RAP binder @ 58°C with 100% RAP binder. ....	51
Figure 26: PAV aged binders of different combination of bio-binder and RAP binder @ 58°C without 100% RAP binder. ....	51
Figure 27: PAV aged binders of different combination of bio-binder and RAP binder @ 64°C with 100% RAP binder. ....	52
Figure 28: PAV aged binders in different combination of bio-binder and RAP binder @ 64°C without 100% RAP binder. ....	52
Figure 29: Sample graph of PG+10°C and PG+20°C frequency sweeps. ....	53
Figure 30: Sample graph of $G'(\omega)$ Master curve at a reference temperature of PG+10°C. ....	54
Figure 31: Relaxation modulus master curve to determine $m_r(60s)$ and $G(60s)$ . ....	55
Figure 32: Relaxation modulus [ $G(60s)$ ] for Unaged binder with high RAP and bio-binder. ....	57
Figure 33: Relaxation modulus [ $G(60s)$ ] for RTFO aged binder with high RAP and bio-binder. ....	58

Figure 34: Relaxation modulus [G(60s)] for PAV aged binder with high RAP and bio-binder. ....	58
Figure 35: Slope ( $m_r$ ) for Unaged binder with high RAP and bio-binder. ....	59
Figure 36: Slope ( $m_r$ ) for RTFO aged binder with high RAP and bio-binder. ....	59
Figure 37: Slope ( $m_r$ ) for PAV aged binder with high RAP and bio-binder. ....	60
Figure 38: Average Rut Depth for different binder combinations with bio-binder and high RAP binder at 58°C.....	62
Figure 39: Average Rut Depth for different binder combinations with bio-binder and high RAP binder at 64°C.....	63
Figure 40: Air void vs rut depth of the specimens tested at 58°C.....	65
Figure 41: Air void vs rut depth of the specimens tested at 64°C.....	65
Figure 42: Sample load-displacement curve.....	66
Figure 43: Sample load-displacement curve.....	67
Figure 44: Average Fracture Energies of different types of HMA mixes. ....	68
Figure 45: Average I-FIT index of different types of HMA mixes. ....	69
Figure 46: Images of failed 100% RAP DCT specimen during preparation. ....	71
Figure 47: Typical Load vs CMOD curve obtained from DCT test. ....	71
Figure 48: Average Fracture Energies for different types of mixtures. ....	72
Figure 49: PG58-28 HMA Mix Design Summary.....	83
Figure 50: PG64-28 HMA Mix Design Summary.....	84

## LIST OF TABLES

Table 1: Amount of Binder Extracted by Solvents.....	25
Table 2: Performance Graded Asphalt Binder DSR specifications (AASHTO M 320)...	31
Table 3: Aggregates gradation collected from Highway-32 Site at ND.....	34
Table 4: Aggregates gradation collected from Interstate-29 Site at ND.....	35
Table 5: Mix design.....	35
Table 6: Relaxation modulus [G(60s)] in MPa for different types of binder with high RAP and bio-binder.....	56
Table 7: Slope ( $m_r$ ) of Relaxation modulus [G(60s)] for different types of binder with high RAP and bio-binder.....	57
Table 8: APA Results Summary @ 58°C.....	61
Table 9: APA Results Summary @64°C.....	62
Table 10. APA Independent T-Test Summary for PG58-28 mixes.....	64
Table 11. APA Independent T-Test Summary for PG64-28 mixes.....	64
Table 12: SCB Fatigue Fracture Energies.....	67
Table 13: SCB Independent t-test Summary.....	70
Table 14: DCT Specimens Fracture Energies.....	71

## **DEDICATION**

To my beloved wife, Doli Rani Saha, who sacrificed her happiness for my study in UND.

To my loving parents who sacrificed everything for me.

## **ACKNOWLEDGEMENTS**

I would like to express my sincere gratitude and appreciation to Dr. Daba Gedafa, P.E., my advisor, for his guidance and support throughout my graduate academic career as well as for giving me the opportunity to work in ND EPSCoR funded project.

I would also like to thank my committee members, Dr. Nabil Suleiman and Mr. Bruce Dockter, P.E. for their valuable support and recommendation to complete this thesis.

I am highly indebted to UND and UND Civil Engineering Faculty for providing all the necessary materials and information necessary for the completion of this thesis.

## **ABSTRACT**

The use of Recycled Asphalt Pavement (RAP) has significantly increased in construction and rehabilitation of flexible pavements to ensure proper utilization of limited natural resources. Recycling also provides a greater environmental benefits and energy conservations. It saves the lands from being the dumping site, conserves energy, and reduces the emission of greenhouse gases. But high RAP in the HMA mix increases the stiffness and may result in cracking. Bio-binders could reduce the stiffness of binder and mixes with high RAP content. Two oils, namely Waste Cooking Oil (WCO), and Soy Oil are potential sources of bio-binder that are abundant and yet to be explored. This research was conducted to explore the effects of selected bio-binders on binder and mixture properties that contain a high percentage of RAP binder. Two different types of aggregates and two virgin binders were used in the study. RAP binder was extracted and modified by the bio-binder. Unaged, Rolling Thin Film Oven (RTFO), and Pressure Aging Vessel (PAV) aged virgin and bio-binder modified RAP binder were tested for both high and low-temperature rheology using Dynamic Shear Rheometer (DSR). Virgin binders were tested as control specimen while 100% RAP binder was used to see the level of modification of RAP binder. These modified binders were further used to make HMA specimens. Nominal maximum aggregate size (NMAS) used for all mixes was 12.5 mm. Eight specimens (150 mm diameter and 75 mm high each) were compacted at a target 7% air void content using gyratory compactor. Asphalt Pavement Analyzer (APA), Semi-Circular Bending (SCB), and Disk-shaped Compact Tension (DCT) tests were conducted to determine the

performance properties of the HMA with modified binder. The results showed that modified binder with bio-binder, virgin binder, and high RAP binder maintained/improved the performance properties of HMA.



# **CHAPTER I**

## **INTRODUCTION**

### **1.1 General**

Pavement is designed to provide adequately strong and durable surface for the smooth movement of traffic during design life. Three types of pavement are generally constructed; asphalt pavement (flexible pavement), concrete pavement (rigid pavement), and composite pavement (combination of flexible and rigid pavement). Asphalt pavement is the predominant type of pavement built in the USA. In the United States, as high as 94 percent of more than 2.7 million miles of paved roads and highways are surfaced with asphalt (NAPA, 2016). Asphalt pavement is a layered pavement system consists of subgrade, sub-base, base, and surface layers. Locally available aggregates (i.e., fine aggregates, and coarse aggregates) are used in the construction of asphalt pavement. Asphalt binders produced from petroleum crude oil are used to glue the aggregates together. Reclaimed Asphalt Pavement (RAP) from old pavement is also used in the construction (Chesner et al., 1998).

### **1.2 Reclaimed Asphalt Pavement (RAP) and Sustainability**

Reclaimed Asphalt Pavement (RAP) is obtained by milling or full-depth removal of the original pavement after service life. It is then processed and reused for pavement construction or dumped as construction debris in a landfill. Recycling of the RAP is the most attractive option for numerous advantages. Usages of RAP in the mix directed

towards the goal of sustainable development, a development that meets the needs of the present without compromising the ability of future generations to meet their own needs” (Brundtland Commission, 1987). It reduces the construction debris placed into landfill and does not deplete the nonrenewable sources of aggregates and asphalt binder. Additionally, recycling provides a greater environmental benefits and energy conservations. It saves the lands from being dumping site while it conserves energy and reduces the emission of CO<sub>2</sub>. Lee et al. (2012) research shown that using 30% RAP in the Hot-Mix Asphalt (HMA) reduces the energy requirement by 16% and CO<sub>2</sub> emission by 20%. The higher the percentage of RAP used in the mix, the higher environmental benefits can be obtained. A relation between environmental benefits with the increase of RAP content in HMA is shown in Figure 1.

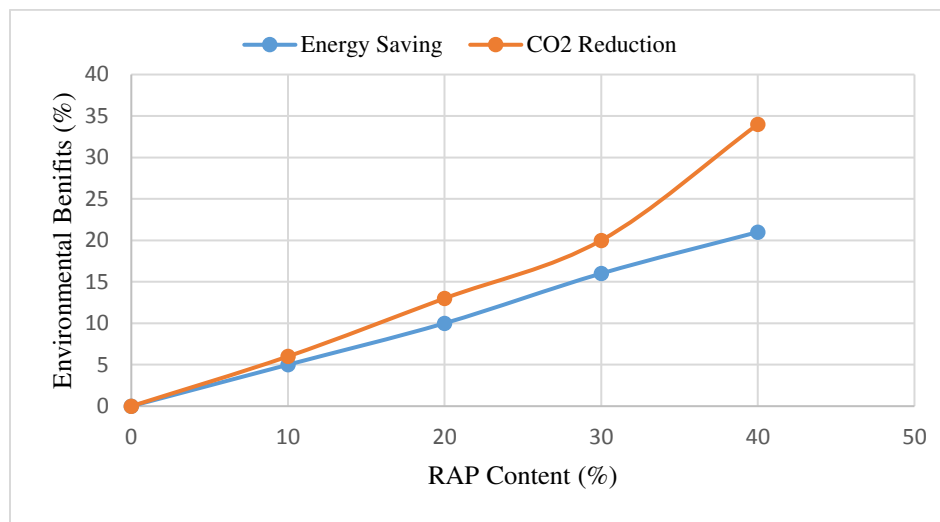


Figure 1: Energy savings and CO2 reduction at different RAP content levels (Lee et al., 2012).

Federal Highway Administration (FHWA), State Departments of Transportation (DOTs) and Environmental Protection Agency (EPA) have given high emphasis for sustainability of transportation systems. To pursue the ultimate goal of sustainable

development, it is the first time the United States enacted a law for surface transportation program called “Moving Ahead for Progress in the 21<sup>st</sup> Century Act” (MAP-21) on July 6, 2012. It is also the first long-term highway authorization enacted since 2005 and funded more than \$105 billion in the fiscal year 2013-2014 for surface transportation programs (FHWA, 2017). One of the important goals stated in the MAP-21 is to establish environmental sustainability, which will pave the way of enhancing the performance of the transportation system while protecting and enhancing the natural environment. Recycling of transportation materials is one of the potential options to achieve this stated goal.

Though RAP usage has numerous advantages, high percentages of RAP (>25%) in HMA is limited due to its effect on the performance properties of the mix. Modification in mix design, as well as modification of asphalt binder, has been explored to maximize the RAP percentage in HMA. Modifying asphalt binder by a bio-binder could be a potential option for incorporating high RAP without compromising much of its performance properties (Alsi et al., 2012).

### **1.3 Bio-binder**

Bio-binders are the oils of low molecular weight hydrocarbon obtained from different sources like agricultural crops, municipal wastes and agricultural and forestry byproducts instead of fossil fuels. Oil collected after the use for cooking termed as Waste Cooking Oil (WCO), and Soy Oil are other sources of bio-binder that are abundant and yet to be explored. These oils can be used in the HMA with or without further processing. The use of the bio-oils can bring economic, social, and environmental advantages. Replacement of asphalt binder partially or fully by bio-oil modified RAP binder from HMA is going to

be a remarkable sustainable practice if the replacement is able to maintain/improve the performance properties of HMA with high RAP (Hill et al., 2014).

#### **1.4 Performance Properties of Asphalt Pavement**

Asphalt pavement encounters three main forms of distresses during service life. These are high-temperature rutting, fatigue, and low-temperature cracking. Rutting is the permanent deformation under the wheel path due to excessively consolidated tire pressure occurred in the early stages of pavement life. Fatigue is the structural failure of the pavement due to repetitive loading that creates alligator type cracking in the pavement. In contrast, low-temperature cracking is a thermal phenomenon which is very common in the northern United States and Canada because of wide ranges of temperature in different seasons and prolonged winter season. Low-temperature cracking causes a transverse crack in the pavement that deteriorates the functional and structural capacity of the pavement. HMA should be designed by paying more attention to these issues (Marasteanu et al., 2007).

#### **1.5 Problem Statement**

While high RAP in HMA promotes sustainable development, its inclusion in high percentages deteriorates the performance of HMA. High RAP in HMA produces a stiff overlay since RAP contains aged binder. Mixes that possess high stiffness are susceptible to fatigue and low-temperature cracking (Mogawer et al., 2012). A better trade off could be achieved by modifying the aged binder. The modification could be done by the addition of bio-binder in optimum percentage. The purpose of this modification is to create a mix that performs well enough against fatigue and low-temperature cracking while maintaining

adequate rutting resistance. This problem statement was investigated to conclude how the rheology of the modified binder and the HMA mix performance properties change.

## **1.6 Objectives**

The objectives of this research are

1. Examine the effect of bio-binder on the rheological properties of modified binder with high RAP binder content.
2. Finding the optimum ratio of RAP binder, bio-binder, and virgin binder that still can provide high performance mix.
3. Analyzing the performance of HMA mix using the optimum ratio of RAP binder, bio-binder, and virgin binder.

## **1.7 Methodology**

Extensive laboratory experiments were done to analyze the effect of bio-binder. The study contains two parts. In the first part, the binder was extracted from RAP materials and the rheology test was performed on extracted RAP binder, RAP binder with bio-binders and virgin binder to see the effect of bio-binders. Based on the results of the rheology test, the optimum ratio of bio-binders, RAP binder, and virgin binder was determined and used to make the mix. HMA specimens were made using the modified binder and tested in the lab to see the effect of bio-binder on the mix properties. To compare the results, control specimens were made using 100% virgin binder. Detail methodology and testing procedures are further explained in Chapter III.

## **1.8 Organization of Thesis**

Chapter I provides information about RAP usage and sustainable development nexus. Chapter II describes the problems of high RAP use in HMA, asphalt binder

chemistry, the potential of using bio-oil in HMA. It also provides further information on the testing for rheological properties of asphalt binders and testing of HMA mix as well. Chapter III describes the experimental plan, RAP binder extraction, binder modification and rheology test, material selection, mix designs, mixing and compaction procedures, and testing procedures. Chapter IV documents the analysis and results of the research. Lastly, the conclusions, recommendations limitations, and future work are included in Chapter V.

## **CHAPTER II**

### **LITERATURE REVIEW**

#### **2.1 General**

High crude oil price, along with greater emphasis given by Federal Highway Administration (FHWA) on sustainability helped to elevate the RAP recycle rate to its highest level in comparison to other materials' in the USA (Hansen & Copeland, 2015). RAP is typically used in various layers of roadway such as base course, intermediate layers, and in the subsurface course. But usage of RAP in the surface course is limited due to the concerns regarding performance properties (Copeland, 2011). A survey conducted by North Carolina Department of Transportation (NCDOT) in 2007, only 10 State transportation departments reported a maximum of 29 percent RAP used in the intermediate layer while less than 5 State transportation departments reported up to 29 percent of RAP used in the surface layer (Copeland, 2011). In 2009, NCDOT again carried out the survey regarding the use of high percentage RAP. DOTs expressed two important concerns regarding the limited use of high RAP in HMA. These are 1) quality of blending between virgin and RAP binder, and 2) stiffness of the resultant mix in the case of high RAP. An overly stiff mix was produced that make the mix susceptible to cracking (Copeland, 2011). Many studies were carried out to mitigate those issues while numerous ideas came out to incorporate more percentage of RAPs in HMA.

## **2.2 High percentage of RAP usages in HMA**

Research works have been done to determine the blending percentage between RAP binder and virgin binder in the mix but found difficult to determine the actual percentage of blending. NCHRP 9-12 study found that at 10% RAP, the black rock (0% blending), total blending (100%), and actual practice were not significantly different. But mixes containing 40% RAP, the black rock case was significantly different from the actual practice and total blending case (McDaniel et al., 2000).

To mitigate the blending effects, superpave specification proposed a blending procedure between RAPs and virgin aggregates to achieve required aggregate structure and volumetric properties of the mixtures. To find the RAP percentage in superpave mix a procedure was proposed where a blend charts of RAP binders and virgin binder were considered (Kennedy et al., 1998). It was a three tier blending procedure where 15% of RAP in the mix was not necessary to change the virgin binder grade for superpave mix design (Bukowski, 1997). In the second tier, 16-25% of RAP in the mix, a lower binder grade (softer binder) by one increment or a rejuvenating agent was suggested. The third tier suggested that RAP percentage beyond 25% in the mix, blending chart was needed to be created for ascertaining the RAP percentage and virgin binder grade. To make the blending chart, the viscosity of recovered RAP binder at different temperatures was determined. This specification assumed that effects of RAP on blended binder properties vary linearly with RAP content. But McDaniel et al. (2006) found in their study that softens the virgin binder grade is not necessarily true to counteract the high stiffness from the RAP binder.



Al-Qadi et al. (2009) did similar kind of study in a different way to see the effects of high RAP in HMA. They performed experiments using extracted RAP binder to determine the percentage of RAP binder blended with the virgin binder and their effects on intermediate and low-temperature performance. They came up with recommendations that up to 20% RAP in the mix, binder grade need not be changed as 100% blend occurred between virgin and RAP binder, while for 40% RAP, double bumping (both high and low-temperature grade) to softer binder is required to achieve the resultant expected binder grade in the final mix. Though rutting resistance was good for a mix of high RAP content, effects of RAP on fracture energy couldn't be offset fully by bumping the binder grade. Moreover, no strong case was observed to support the approach of using a softer-grade virgin binder for high RAP mixes from field performance data obtained from the National Center for Asphalt Technology (NCAT) test track and also from the results of a variety of laboratory tests (West et al., 2009).

In addition to blending concern, HMA mixture stiffness with RAP is high and as the RAP increases, the stiffness of the mix also increases (Valdes et al., 2011). This overly stiff mix is produced due to the aged binder content in the RAP. Asphalt binder loses its strain tolerant properties during the aging process. Hence, the stiffer mix is highly susceptible to all types of cracking. A mix with 50% RAP blend showed the lowest fatigue resistance compare to virgin mix and mix with rejuvenator (Tran et al., 2012). Colbert and You (2012) found that addition of RAP binder increased the resilient modulus by 52%, which stiffens the mixture under higher temperature and heavier loading condition.

The rejuvenating agent was introduced in HMA with high RAP for improving the properties against cracking. Purposes of the uses of the rejuvenating agent in HMA with

high RAP was to regain the chemical and mechanical properties of the RAP that were lost during aging. Softer grade binder could also be used as rejuvenator which provides flux oil and lube stock to RAP mix. Usage of rejuvenator in a low percentage (< 10% of RAP) in the mix with 15%, 38% & 48% RAP was able to improve the indirect tensile strength and rutting resistance (Shen et al., 2007). However, State agencies put a restriction on the use of rejuvenator in HMA due to poor rutting performance and requirement of additional equipment. Modification of RAP binder to regain the lost properties of aged binder could be a potential solution for incorporating the high RAP. Analysis of asphalt chemistry will pave the way of modification of RAP binder.

### **2.3 Asphalt Chemistry**

Asphalt has been generally used for roads and highways construction for a long time due to its adhesive properties. It was first found in Lake naturally but the quantity wasn't enough to meet the ever increasing demand (NAPA, 2016). To catch the pace of increasing demand, petroleum asphalt has been produced. It's a byproduct of petroleum crude oil obtained by the fractional distillation process. The chemical composition of asphalt is extremely complex in nature which contains a lot of organic and organic-metallic components. Difficulty in defining the exact chemical composition lead Read and Whiteoak (2003) to group the chemical components of asphalt into two categories. These two main chemical component groups are Asphaltenes and Maltenes. Maltenes further subdivided into three other components- Saturates, Aromatics, and Resins. Asphaltenes are polar compounds with high molecular weight that provide viscous properties to the asphalt. On the contrary, maltenes are the lower molecular weight oily medium where asphaltenes are dispersed.

Rheological properties of the asphalt mainly depend on the quantity of asphaltenes present in the asphalt cement. Asphaltenes to maltenes ratio in asphalt binder is changing over time due to environmental effects, fatigue, etc. The presence of high asphaltenes in the asphalt makes it harder and stiffer. During the aging and oxidation process asphalt losses its maltenes hence the ratio of asphaltenes to maltenes increases and the asphaltenes flocculate, consequentially a stiffer binder formed. When it is used in the HMA, it creates a stiffer mix that makes the mix susceptible to low-temperature cracking (Tyrion, 2000).

## **2.4 Bio-Oil**

There are several bio-oils found by the researchers retrieved from biomass materials such as waste wood, swine manure, from corn stover, tea and coffee residue, rapeseed and soybean etc. Some other bio-oils are also available from recyclable sources like Waste Cooking Oil, Soy Oil, etc. Bio-oil contains the low molecular weight hydrocarbon compound. As aged RAP binder loses its maltenes part during aging, the ratio of asphaltenes to maltenes in the binder is increased. The addition of bio-oil in optimum level can increase the maltenes part of the aged binder and restore the asphaltenes to maltenes ratio in the resultant binder. Moreover, WCO and Soy Oil are a good recyclable source and proper use of these oils for sustainable pavement will be helpful.

### **2.4.1 Waste Cooking Oil (WCO)**

Waste Cooking Oil (WCO), also known as Used Cooking Oil (UCO) is abundant in the metropolitan area due to the presence of lots of hotel and restaurant. These hotels, restaurants and fast food establishments dump the oil after frying and cooking. The amount of dumped WCO in the United States is approximately 3 billion gallons per year (EPA, 2017). Dumping of WCO is ending up in a landfill, municipal sewer pipe, and eventually

in water bodies that cause negative impacts on the environment. Researchers have been trying to explore the potential area to reuse WCO that only ensure a better alternative use but also reduces the environmental pollution from illegal dumping into water bodies. Bio-diesel (EPA, 2017), bio-asphalt (Wen et al., 2013) are some potential area discovered for the recycling of WCO. Bio-asphalt is produced from WCO by a thermochemical process where WCO has to undergo the polymerization process at elevated temperature. Uses of bio-asphalt in HMA mix with base binder reduce the stiffness of the mix which improves resistance to thermal cracking properties of the mix (Wen et al., 2013). WCO can also be used directly without any further chemical changes. The presence of high percentage of lower molecular weight oily medium (maltenes) in WCO can possibly make it as a rejuvenating agent for aged RAP binder with lower maltenes. The addition of WCO in the RAP binder decreases the ratio of asphaltenes to maltenes in the RAP binder due to the increase of maltenes that constitute the WCO (Alsi et al., 2012). The addition of WCO further improves the rheological properties of the aged binder presence in RAP (Zargar et al., 2012).

#### **2.4.2 Soy-Oil**

Vegetable-based materials, such as soy, are appealing as flexible pavement materials because of their short-term renewable nature and hydrocarbon chemical structure. It may be plausible technically, economically, and environmentally for soy fatty acids (SFAs) from soapstock to serve as a paving asphalt additive at low modification levels. Rheological tests show that as SFAs are added in small percentages, the binder becomes less stiff and more workable. These results suggest that SFAs have potential application as

a flexing agent for binders that are stiff and hard to mix, such as RAP binder (Seidel and Haddock, 2012).

## **2.5 Binder Rheology**

Rheology is the study of flow and deformation of matter mainly in a liquid state. It is the measurement of the resultant stress or deformation on the materials after applying strain. The rheology is also temperature dependent. Wide ranges of temperature from low to high are used to measure the properties. Rheological properties are used to characterize the viscoelastic properties of materials. Asphalt is considered as a viscoelastic material (Read and Whiteoak, 2003). It is a semi-solid material at room temperature and behaves like elastic material. But in high temperature, it turns into a viscous liquid that flows easily. Deformation and flow of asphalt binder are important in HMA pavement performance. Intuitively it can be said that binder with higher flow ability or deform more are susceptible to rutting while low flow ability is one of the important causes of fatigue cracking (Pavement Interactive, 2017).

Three cases are considered for the asphalt binder rheology test as virgin binder undergoes two types of aging during the service life, 1) short-term aging and 2) long-term aging. Short-term aging occurs during mixing and construction mainly due to the volatilization and absorption of oily components in the maltenes. Long-term aging occurs during the service life in the field due to changes in composition through a reaction between asphalt constituents and atmospheric oxygen, a chemical reaction between molecular components (polymerization), and formation of a structure within the asphalt binder (thixotropy) (Roberts et al., 1996). Short-term aging of asphalt is simulated in the laboratory by Rolling Thin Film Oven (RTFO) test while long-term aging is simulated by

Pressurize Aging Vessel (PAV) test. Temperature is controlled during testing in medium- and-high temperature and low-temperature.

### **2.5.1 Medium and High-Temperature Rheology**

The most common method used to determine the binder rheology is Dynamic Shear Rheometer (DSR) test. This test measures the viscous and elastic behavior of the binder, as represented by the complex shear modulus ( $G^*$ ) and phase angle ( $\delta$ ), respectively (Wang et al., 2011). DSR shows the asphalt binder's resistance to permanent deformation (high-temperature) and fatigue cracking (medium-temperature). Permanent deformation resistance is measured on the unaged and RTFO-aged asphalt binders, and the fatigue cracking is measured on the PAV-aged asphalt binders (Seidel and Haddock, 2012).

### **2.5.2 Low-Temperature Rheology**

Low-temperature rheology of asphalt binder is the predominant factor to control the low-temperature performances of asphalt pavements. Bending Beam Rheometer (BBR) has been used for several decades to test asphalt binders at low-temperatures to determine their susceptibility to thermal cracking. There are some other methods i.e., Direct Tension Test (DTT) and Torsion Bar (TB) that have also been used sometimes. However, a relatively large amount of asphalt binder requirement makes this difficult to apply to extracted asphalt binder; relatively high temperatures (above 135°C) lead to difficulties in preparing specimens, and these are time-consuming in terms of molding the test specimens.

Sui et al. (2011) proposed an alternative low-temperature test to BBR that enables determination of low-temperature performance grade which only requires approximately 25 mg of asphalt binder to perform a test. The test employs 4-mm diameter parallel plates on a DSR and includes a correction for machine compliance allowing testing to -40 °C. In

the method, a correlation was developed to find the BBR  $m$ -value and creep stiffness  $S(t)$ . This method was further modified which incorporated Time Temperature Superposition (TTS) (Farrar et al., 2015). By this superposition, a master curve was generated at a reference temperature of PG+10°C using two frequency sweeps at PG+10°C & PG+20°C. Slope ( $m_r$ ) and relaxation modulus  $G(t)$  at 60 seconds are estimated from the  $G(t)$  master curve at the PG+10°C. It has been demonstrated that this new technique is a reliable, fast, and simple test method to obtain low-temperature rheology of asphalt binders (Sui et al., 2011).

## **2.6 Cracking potential of HMA and Tests**

Cracking is one of the most important distress of asphalt pavement that deteriorates the pavement structural and functional capacity. Usages of aged RAP materials in the HMA make the pavement more susceptible to raveling and cracking especially reflective cracking due to the brittleness of the aged asphalt binder (Lu and Isacsson, 1998). Fracture mechanics has been applied to explore the mechanism of crack in asphalt concrete from long ago and has become popular in the research community (Kim and El Hussein, 1995; Jacobs et al., 1996). Nonlinear fracture mechanics approach determines the fracture energy ( $G_f$ ) of asphalt pavement. Fracture energy can be defined as the amount of work to create a new surface or crack of unit length (Bazant and Planas, 1997). Chiangmai (2010) suggested that fracture energy found by nonlinear fracture mechanics approach is the most appropriate parameter to describe asphalt concrete fracture. This study also recommended that total fracture energy is the most promising parameters for the prediction of fatigue behavior. Mixes that can tolerate high strains before failure showed high fracture energy and are more likely to resist cracking compare to the mixes with low strain endurance. There are several methods based on fracture mechanics principle to determine the fracture

energy of the HMA mix. The commonly used methods are Disk-shaped Compact Tension (DCT) test and Semi-Circular Bending (SCB) test.

## **2.7 Intermediate Temperature Cracking and SCB Test**

Semi-Circular Bending (SCB) test is a three-point bending test using semi-circular geometry based specimen with a notch in one edge. The principle of the test is based on fracture mechanics approach that calculates the total fracture energy of the specimen. SCB test is a simple and low-cost test that can be easily performed on the cylindrical sample obtained from standard specimens prepared in the superpave gyratory compactor. Several standard methods for the test are available such as test at Intermediate temperature by ASTM: D8044-16 (ASTM, 2016) and SCB test at Intermediate temperature by AASHTO: TP 124-16 (AASHTO, 2016). The former standard method gives strain energy to failure using a specimen thickness of 57mm at an intermediate temperature (calculated using avg. of binder PG high and low-temperature) while later method gives Flexibility Index (FI) in addition to fracture energy using a specimen thickness of 50mm at 25°C. FI is a dimensionless index derived from the load-displacement curve obtained from SCB test. The value of the index depends on the fracture energy, crack propagation growth, and post-peak slope of the load-displacement curve (Ozer et al., 2016).

A typical load-displacement curve obtained from SCB test is shown in Figure 2. FI index is calculated from the curve using Eq.(2.1).



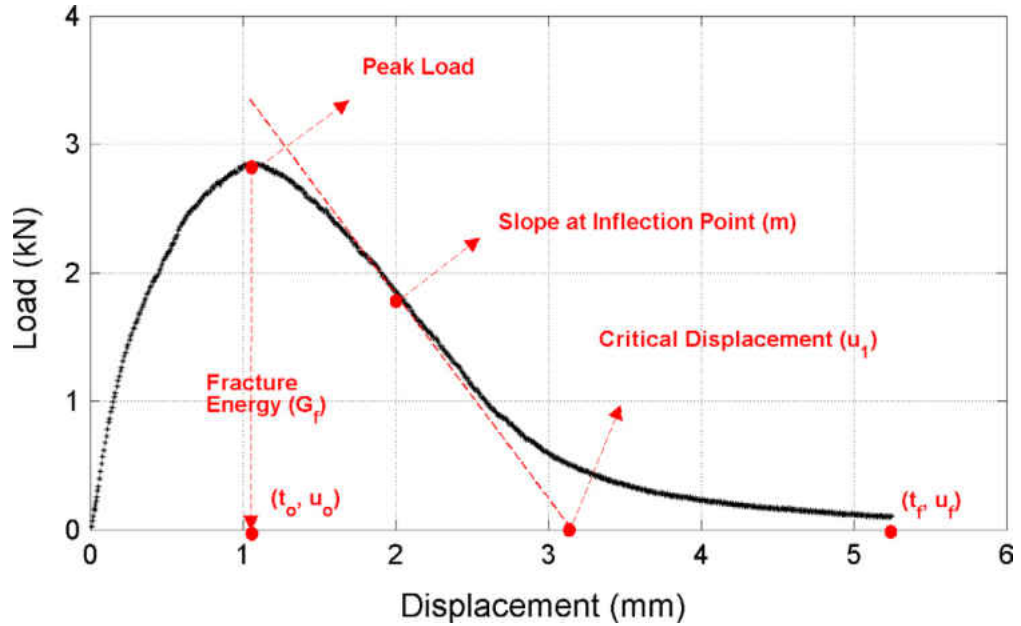


Figure 2: Typical Load-Displacement curve obtained from SCB test (Ozer et al., 2016).

$$FI = A * (G_f / |m|) \dots \dots \dots Eq.(2.1)$$

Here,

$G_f$  = Fracture energy found from the area under the curve.

$m$  = slope of the curve at inflection point after peak load.

$A$  = Conversion factor

FI index is used to categorize the AC mixture from brittle to ductile based on the crack propagation growth. A higher value of FI denotes the better performing asphalt pavement. Ozer et al. (2016) suggest that best performing AC mix has FI values greater than 4.5, poor performing AC mixes have FI value less than 2 and intermediate performing category lies in between them. This index is also efficient due to its simplicity and good correlation to crack propagation growth

## **2.8 Asphalt Pavement Low-Temperature Cracking and DCT Test**

Low-temperature cracking or thermal cracking of asphalt pavement is the tensile strain induced cracking due to the drop in the temperature to a critically low level. It is the predominant distress of asphalt pavement in the northern United States and Canada due to prolonged cold winter season. Though this is an environmental issue rather than traffic loading, it can also be happened from fatigue because of freezing and thawing cycles. Low-temperature cracking is a top-down cracking, initiated at the top of the pavement and propagates to the bottom (Brown et al., 2001). Major factors considered for this type of cracking are stiffness of the mix in addition to the magnitude and frequency of low-temperature on the surface (Brown et al., 2001).

Several test methods based on fracture mechanics are available to evaluate the low-temperature cracking resistance of HMA specimen in the lab. Specified low-temperature is used to measure the fracture energy. Variation of the results is occurred based on testing temperature and size of the specimen. Commonly used temperature is low-temperature PG+10°C. Two most widely used low-temperature test methods are SCB and DCT. However, SCB is highly recommended for intermediate temperature cracking test (Ozer et al., 2016). In contrast to SCB test, DCT test has the capability to capture the transition of asphalt concrete from a brittle material at low-temperatures to a more ductile material at higher temperatures (Wagoner et al., 2005). The valid temperature range they found was -20°C to 0°C that simulates the northern United States average low-temperature.

## **2.9 Asphalt Pavement Rutting**

Rutting is another asphaltic pavement's distress which is likely to occur in the early stages of a pavement's life. This is a high-temperature phenomenon of asphalt pavement

and unique distress for this pavement type because of having flexibility in contrast to the rigidity of concrete pavement. Permanent deformation on the pavement under wheel path termed as rutting that's occurred due to excessively consolidated tire pressure applied by traffic. Rutting may occur due to an issue with the HMA layer, base or subgrade. Lack of proper compaction in base or subgrade layer sometimes causes the rutting. But insufficient mixture stability is considered as the underlying cause of rutting. Consolidated repetitive traffic load creates this plastic deformation on the pavement which causes the functional and structural failure of the pavement (Khedr and Breakah, 2011).

Different mix design parameters have the effects on rutting such as Fine Aggregate Angularity (FAA), PG grade of Asphalt, etc. Higher PG grade binder or higher percentage of FAA has better resistance to rut for same passes of wheel loads (Suleiman, 2008). The addition of RAP in HMA also has an effect on rutting. RAP produces a stiff mix that improves the rutting resistance of the mix (Shen et al., 2007; Van Winkle, 2014). But binder modification by bio-oil or by rejuvenator reduced the rutting resistance of the HMA mix with RAP (Shen et al., 2007).

## **2.10 Bio-Oil modified binder and mix with High RAP Binder**

Based on the asphalt chemistry, aged binder loses its maltenes part thus increase the ratio of asphaltenes to maltenes in the resultant binder. The addition of low molecular weight oil can be able to balance the ratio in the aged asphalt and to reconstitute its rheological properties. Reconstitute aged binder could be able to replace the virgin binder by a high percentage. Moreover, WCO and Soy Oil are available in abundance which creates environmental hazards. While usages of these oil in asphalt pavement is a better alternative to promote sustainability in all way by saving the environment, energy, and

cost. But this dimension of research yet to be explored. Though few studies regarding the usages of WCO for regaining the properties of asphalt binder occurred, the novelty of this research sees the effect of both WCO and Soy Oil in a binder for high-and-intermediate temperature and low-temperature. Furthermore, the reconstitute binders were used to make specimen in the lab and tested to characterize its cracking and rutting potential while cracking potential was measured for both high and low-temperature to simulate the prevailing the field condition of northern United States, especially in North Dakota.

## **CHAPTER III**

### **METHODOLOGY**

#### **3.1 Experimental Plan**

An extensive laboratory experimental plan was made to do the study. The plan consists of two phases of the experiment. The first phase was all about asphalt binder testing and modification while the second phase was to make the specimen using that binder and testing. Steps of the phases are shown in Figures 3 and 4. In the first phase, RAP binder was extracted from the RAP materials using a solvent. Rheological properties of the RAP binder and virgin binder were tested. In addition to that RAP binder was modified with bio-oil and virgin binder to find the optimum combination. It is a trial and error process. There were thousands of possibilities of combining RAP binder with bio-oil and virgin binder. But the main purpose of the study was to maximize the use of RAP and bio-oil. Several combinations were tested in DSR to observe the rheological properties and compare it with a virgin binder. Optimum combinations were determined to be used the second phase testing. HMA mix specimen test is very important to verify the performance of the mix as well as the performance of the binder. Determining mix performance is critical since there are some other factors, such as adhesive and cohesiveness of the binder, binder interaction with aggregates, drain down characteristics of the binder in the mix, etc. that can affect mix performance. Therefore, in the second phase, HMA mix was prepared using the optimum combinations of modified binder. Superpave gyratory compactor was

used to make the specimens. Volumetric properties were then cross-checked with the Superpave specification. After that, specimens were tested for determining the resistance against three important distresses. First, the specimen was tested for high-temperature rutting resistance using APA machine. Then the specimens were cut using a diamond cutter and diamond drill to make the specified size of the sample for DCT and SCB tests. DCT test was performed to test low-temperature cracking resistance while SCB test was done to check the intermediate temperature fatigue cracking resistance. For all cases, control specimens were made using 100% virgin binder.

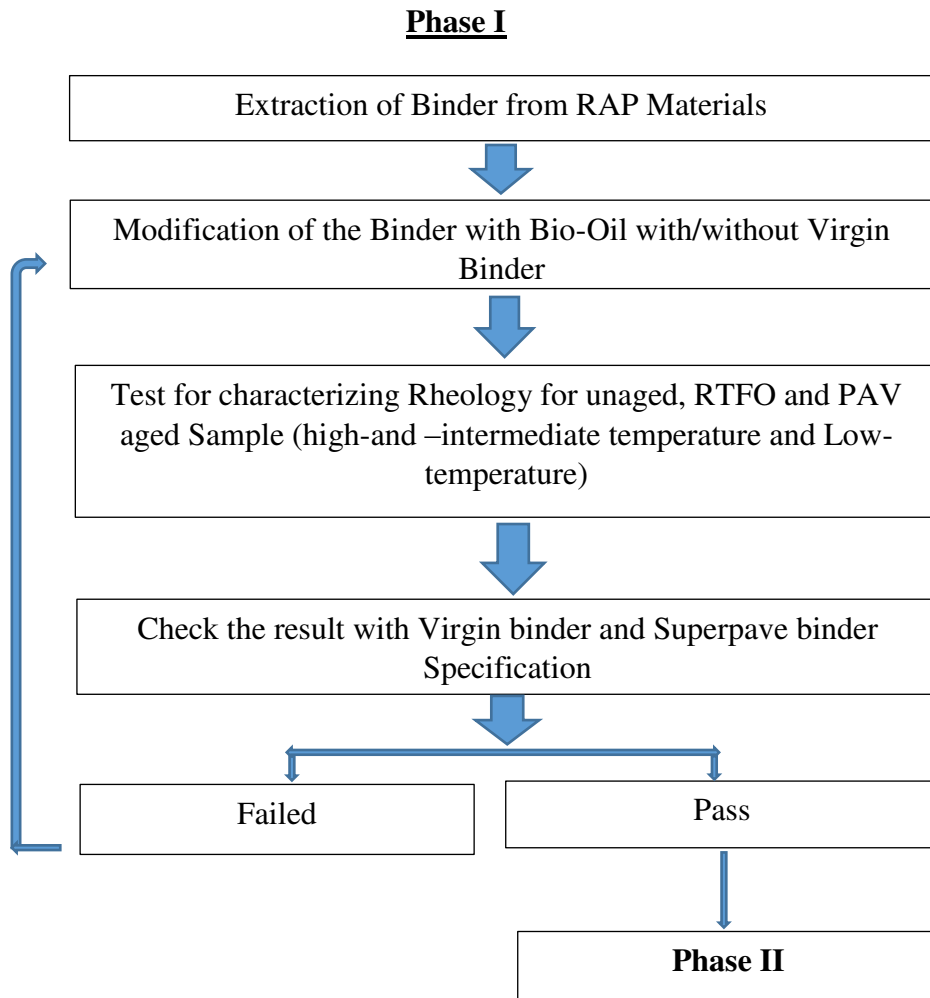


Figure 3: Flow Chart of Phase I test plan.

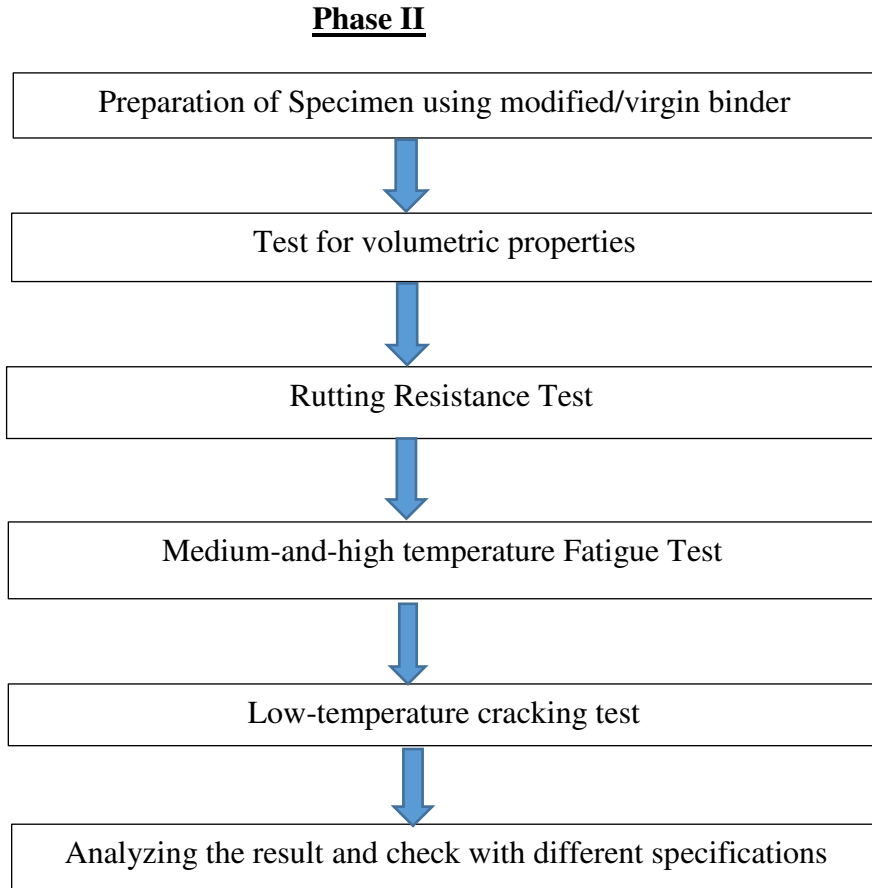


Figure 4: Flow Chart of Phase II test plan.

### **3.2 Materials Selection**

Two different types of materials were collected from the two different construction sites. One was North Dakota State Highway-32 construction while another was Interstate-29 (I-29) construction in North Dakota. Two virgin asphalt binders of Superpave grade PG 58-28 and PG 64-28 were selected for the study as it is recommended for the highway in Midwest of USA considering its temperature variation. PG 58-28 was used with materials collected from Highway-32 site whereas PG 64-28 was used with the materials collected from the I-29 site. In original mix design, RAP was used for both cases and the percentage were 24% and 22% for Highway-32 and I-29, respectively. RAP sources were also different for both cases. RAP used for Highway-32 was collected from roadway which was

originally paved in 2005 using binder grade PG 58-28 while RAP collected for I-29 from roadway which was originally paved in 2004 using the same binder grade. RAP binder used in this study was extracted from these RAP materials using a chemical solvent in the laboratory. Selection of solvent and extraction procedure is discussed in Section 3.3.

### **3.3 RAP Binder Extraction and Selection of Solvent**

RAP binder used in this research was extracted from the collected RAP material in the laboratory. It is a two-stage recovery process that comprises binder removal from aggregate using a solvent and then retrieved the binder from the solvent. Solvent selection for this process is a tricky one as several solvents are available in the market. Health and environmental hazards are the major concern while extraction efficiency is also considered for the final selection of the solvent. Due to hazardous nature of chlorine based solvents, many researchers used non-chlorinated solvent, or a bio-degradable solvent in a centrifuge, reflux, or vacuum extractor. Solvents are ranked by their comparative human toxicity as follows: Trichloroethylene (TCE) > Perchloroethylene (PCE) > Isopropyl Bromide (iPB) > stabilized nPB/nPB (Stelljes, 2001). N-Propyl Bromide (nPB) is a non-chlorinated solvent that has been classified as noncarcinogenic and non-hazardous. The use of nPB for asphalt extraction and the implementation of nPB on-site recycling would generate only non- hazardous still bottom waste (McGraw et al., 2001). The NCHRP 9-12 research project showed that nPB could be used as an extraction solvent without affecting asphalt binder contents and binder properties (McDaniel, Shah, Huber, & Gallivan, 2007). The U.S. EPA has approved nPB under the Significant New Alternatives Policy (SNAP) as a suitable replacement for ozone depleting chemicals (Enviro Tech International, Inc, 2008). Research done for the Florida Department of Transportation found that Solubility and



Extraction testing with different asphalts also showed no statistical difference between using TCE on extraction results. It has been recommended that fresh nPB be used when recovering asphalt for binder testing. nPB solvent extractions took less time than the TCE extractions. Researchers concluded that nPB could be substituted for TCE as an extraction solvent without change to current test methods (Collins-Garcia et al., 2000).

EnSolv is one the nPB solvents. The results for the extraction and recovery process showed that EnSolv and recovered EnSolv from the standpoint of extraction would be a suitable replacement for TCE. The EnSolv and recovered EnSolv were also shown to require less time to complete the recovery process than TCE. Viscosities of all recovered binders from both solvents were comparable (Burr et al., 1991).

Three different types of solvents were used to extract binder from RAP: EnSolv-EX, EnSolv-NEXT, and TCE. EnSolv-EX and EnSolv-NEXT do not have flash points, which mean they are safer.

RAP binder whose original grade was PG 58-28 was extracted using the three solvents. Table 2 shows the amount of binder extracted by the three solvents. EnSolv-EX is the most efficient solvent since the binder extracted is the maximum and EnSolv-NEXT is the least efficient, but initially, more RAP was used in the case of EnSolv-NEXT and it may have an impact on the amount of binder that is extracted from RAP. EnSolv-EX was selected to extract all the binders from RAP to determine rheological properties in this study.

Table 1: Amount of Binder Extracted by Solvents.

<b>Solvent</b>	<b>Initial Weight (g)</b>	<b>Final Weight (g)</b>	<b>% Binder Recovered</b>
EnSolv-EX	250	238.4	4.64
TCE	200	194.7	2.65
EnSolv-NEXT	1000	975	2.5

Extraction of RAP was done in the laboratory following the ASTM D 2172/D 2172M standard (ASTM, 2011) and ASTM D 1856-95a Standard (ASTM, 2003) procedure jointly. EnSolv-EX is an n-Propyl Bromide (nPB) solvent which was used in this extraction. According to ASTM D 2172/D 2172M procedure, 1000 gm of RAP aggregates was placed in a bowl is shown in Figure 5. 200 ml of the aforementioned solvent was added to the mixture and started the centrifuge revolving. It was started slowly and gradually speed up to a maximum of 3600 rev/min. The drained down solvent with RAP binder was then collected in a jar. This process was repeated for 3-4 times.



Figure 5: Extraction Bowl Unit (ASTM, 2011).

RAP binder from this extracted solvent was then recovered following ASTM D 1856-95a Standard procedure by Abson Method. It is a fractional distillation procedure which has been used since the early 1930s and is effective in the removal of the majority of the solvent from the asphalt binder (Abson and Burton, 1960). The essential apparatus

used for this extraction are shown in Figure 6. Extracted solvent collected from the previous process was taken to a distillation flask of 250-ml size. Electric heating was introduced and continued until the temperature reaches 135 °C (275 °F). The EnSolv-EX solvent was vaporized from the mix and came out through a funnel, condensed inside the funnel and dripping in a jar. The residue in the flask was the RAP binder and collected for test and another purpose. During the process, for agitating the process and preventing foaming inside the flask, Carbon-di-Oxide (CO<sub>2</sub>) gas was introduced. The whole process from extraction to the recovery of asphalt binder was finished within 8 hours as specified in the standard.

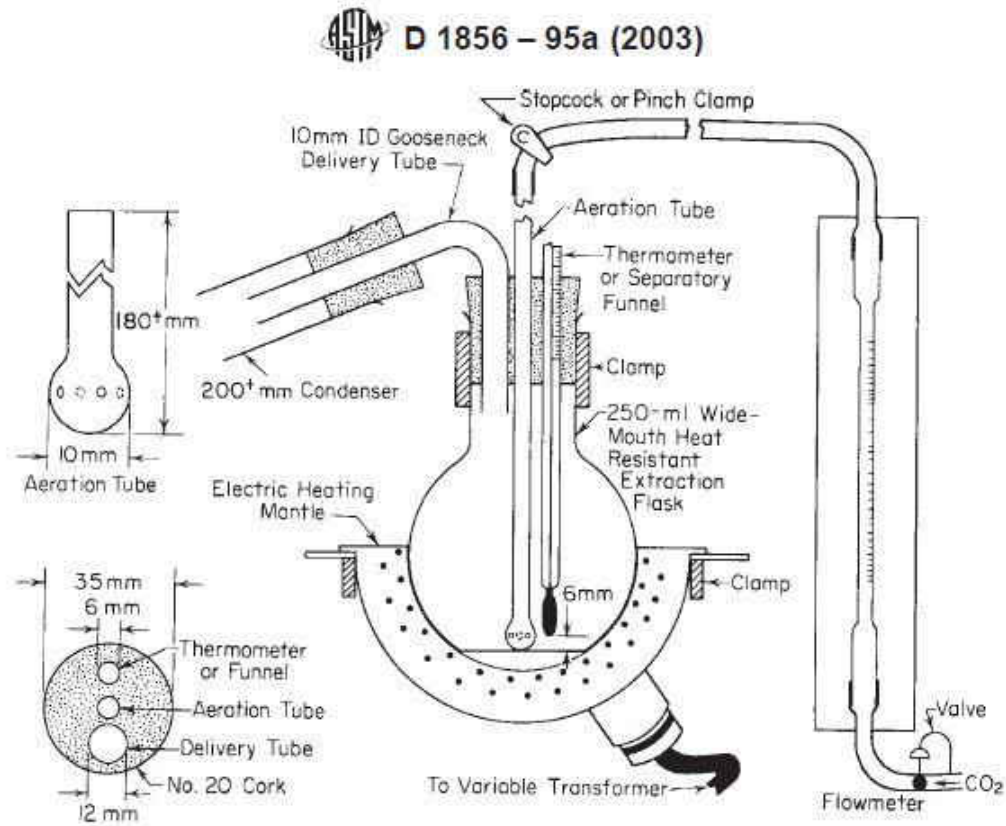


Figure 6: Fractional Distillation Unit by Abson Method (ASTM, 2003).

### 3.4 Dynamic Shear Rheometer (DSR) Test

Rheological properties of the virgin binder and modified binder were tested using Dynamic Shear Rheometer (DSR) manufactured by Anton Paar Inc. The machine is synchronized with a computer software for running the test. High and intermediate temperature rheology was tested following ASTM D7175 standard (ASTM, 2008) method. Both rutting and fatigue parameter were tested. For rutting resistance measurement, unaged and RTFO aged binder were used while PAV aged binder was used to determine the fatigue resistance of the binder. The diameter of the specimen used in the test was 25mm which was made by pouring the annealed hot asphalt into a 25mm silicon mold. After cooling down of the sample it was transferred to the lower plate of the machine. Strain rate and frequency used for amplitude sweep were 10% and 10 rad/sec respectively. The machine setup for DSR high and medium temperature test is shown in Figure 7.



Figure 7: DSR test setup.

DSR test provides complex shear modulus ( $G^*$ ) and phase angle ( $\delta$ ) of the binder. The complex shear modulus is related to the strength of material whereas the phase angle provides the information about the ratio between viscous and elastic response during the shearing process. The applied shear stress and resulting shear strain on the sample during DSR test are shown in Figure 8. Both the viscous and elastic portion of the material with phase angle and complex shear modulus are shown in Figure 9. From the figure, it is observed that larger phase angle denoted more viscosity of the materials.

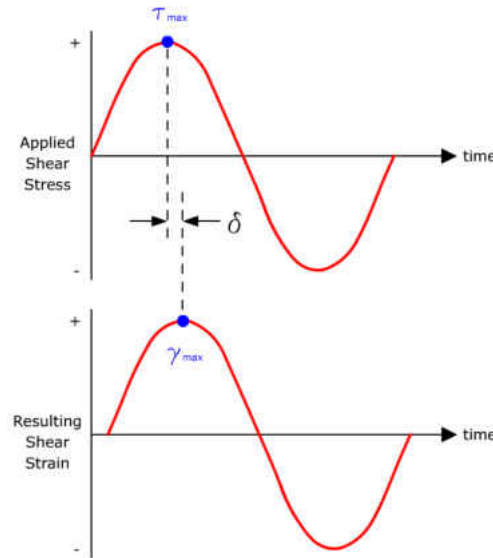


Figure 8: Applied Shear Stress and Resulting Shear Strain on Asphalt (Pavement Interactive, 2016).

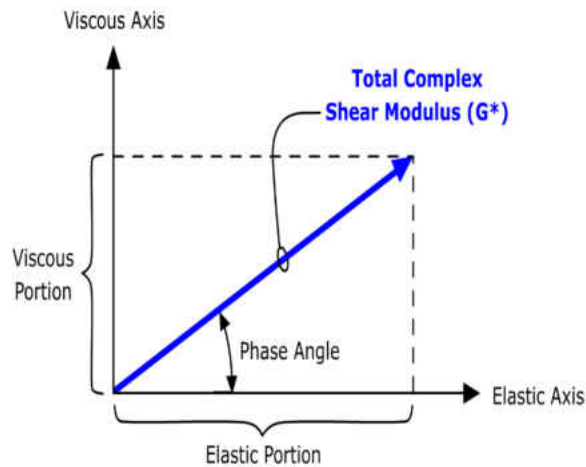


Figure 9: Complex Shear Modulus (Pavement Interactive, 2016).

DSR Superpave specifications of binder for rutting and fatigue were made based on these complex shear modulus ( $G^*$ ) and phase angle ( $\delta$ ) data. For each loading cycle on the pavement surface, a work is being done to deform the pavement surface. Part of this work is recovered by the elastic rebound of the pavement surface while the other part is dissipated in the form of permanent deformation, heat, and crack propagation etc. Dissipated energy per loading cycle is expressed in the Eq.(3.1) (Pavement Interactive, 2016).

$$W_c = \pi\sigma_0^2 \left[ \frac{1}{G^* \sin \delta} \right] \dots \dots \dots \text{Eq.(3.1)}$$

Where,

$W_c$ = Work dissipated per load cycle.

$\sigma_0$ = Stress applied during the load cycle.

$G^*$ = Complex Shear Modulus.

$\delta$  = Phase Angles

Minimizing the dissipated work per load cycle reduces the permanent deformation/rutting on the pavement surface. From equation 3.1, it is seen that maximizing the value of  $G^*/\sin(\delta)$  minimize the work dissipated. Hence for rutting, a minimum value is specified.

On the other hand, fatigue is governed by the applied strain on the pavement surface. The dissipated work per loading cycle is expressed in the Eq.(3.2).

$$W_c = \pi \epsilon_0^2 [(G^*)(\sin \delta)] \dots \dots \dots \text{Eq.(3.2)}$$

Where,

$\epsilon_0$ = Strain applied during the load cycle.

Minimizing the dissipated work per load cycle reduces the crack propagation/fatigue cracking on the pavement surface. From equation 3.2, it is seen that minimizing the value of  $(G^*)\sin(\delta)$  minimize the work dissipated. Hence for fatigue cracking, a maximum value is specified.

Low-temperature rheology of the binder was also tested using the DSR machine. A method was proposed by Sui et al., (2011) which was further modified by Farrar et al., (2015). This method was applied to generate the master curve at low-temperature PG+10°C. The master curve was then used to estimate the slope ( $m_r$ ) and relaxation modulus  $G(t)$  at 60 seconds. Finally, these values were compared to Superpave PG binder specifications that are shown in Table 2.

Table 2: Performance Graded Asphalt Binder DSR specifications (AASHTO M 320).

Material	Value	Specification	Distress of Concern
Unaged binder	$G^*/\sin\delta$	$\geq 1.0$ kPa (0.145 psi)	Rutting
RTFO residue	$G^*/\sin\delta$	$\geq 2.2$ kPa (0.319 psi)	Rutting
PAV residue	$G^*.\sin\delta$	$\leq 5000$ kPa (725 psi)	Fatigue cracking

Creep Stiffness, following AASHTO 313, 'S', maximum of 300 MPa and Slope ( $m_r$ ) value, minimum of 0.300 @ 60 seconds.	Low-Temperature Cracking
--------------------------------------------------------------------------------------------------------------------------	--------------------------

### 3.5 Rolling Thin Film Oven (RTFO) Test

Modified and non-modified asphalt binders were aged by following RTFO test procedure to simulate short-term aging during mixing and placement. This test was performed according to ASTM D2872-04 (ASTM, 2004) standard procedure. The oven used for RTFO test is shown in Figure 10.



Figure 10: RTFO oven.

It is a double-walled electrically heated convection-type oven. The oven was pre-heated for 16 hours prior to the testing to stabilize the testing temperature at  $325 \pm 1^\circ\text{F}$ . Firstly, the binder was heated to a maximum of  $302^\circ\text{F}$  in a loosely fitted container before pouring into a cylindrical glass container. In each container,  $35 \pm 0.5$  g of the binder was



poured then, turned to a horizontal position and immediately rotated for at least one complete rotation for pre-coating the cylindrical surface. These containers are allowed to cool down for 1 to 3 hours. After cooling period, the containers then placed into the preheated oven for the test. The test was done at a temperature of  $325 \pm 1^\circ\text{F}$  and airflow of  $4000 \pm 200 \text{ mL/min}$ , for 85 minutes. After the test sample was collected in a silicon mold for rheological test and the residue was used for further aging in PAV.

### **3.6 Pressurized Aging Vessel (PAV) Test**

RTFO residue was used to do PAV test that simulates 7 to 10-years of binder aging during service life exposed to the dynamic environment. The test was performed by following ASTM D6521 – 08 standard test procedure. Testing temperature was  $100^\circ\text{C}$  that was selected by following ASTM D6373 – 99. The PAV vessel used for the test is shown in Figure 11.



Figure 11: PAV vessel.

The vessel was preheated to 95°C before loading the sample into the vessel. An amount of 50 ± 0.5 g of RTFO aged binder was poured into the stainless steel pan then placed into the preheated vessel. The test was run for 20hrs at a temperature of 100°C and a pressure of 2.10 ±0.1 MPa. Finally, PAV aged sample was collected in a silicon mold for DSR test.

### 3.7 Mix Design

Two different mix designs were used for HMA mix in this study. These two mix designs were unique in many cases such as in one design PG 58-28 binder was used while in another one PG 64-28 binder was used. Mix design with binder PG 58-28 was used for the Highway-32 and mix design with binder PG 64-28 was used for the I-29 construction. Both mix designs were provided by the mix design technician, Danny Schmidt. Aggregates gradation, blending and other important properties of the mix are given in Table 3-5. RAP was fractioned and included in the original mix design. But in this study, for the control sample and all other samples in which modified binder was used, RAP material was excluded and an additional proportion of aggregates were added by analyzing the gradation of the RAP in each performance grade. Nominal Maximum Aggregate Size (NMAS) used in both mix designs was 12.5 mm.

Table 3: Aggregates gradation collected from Highway-32 Site at ND.

	N Fines	Rock	Washed Dust	Dirty Dust	Lower Control Pt	Upper Control Pt
Sieve Size	% Passing	% Passing	% Passing	% Passing	% Passing	% Passing
5/8" (16mm)	100	100	100	100	100	100
1/2" (12.5mm)	100	92	100	100	90	100
3/8" (9.5mm)	99	62	100	100		
#4 (4.75mm)	83	3	86	93		

#8 (2.36mm)	65	1	45	68	28	58
#16 (1.18mm)	45	1	26	47		
#30 (0.6mm)	23	1	14	33		
#50 (0.3mm)	8	1	7	23		
#100(0.15m m)	6	1	4	16		
#200(0.075m m)	4.5	1	2.1	12.7	2	7
Pan	0	0	0	0	0	0

Table 4: Aggregates gradation collected from Interstate-29 Site at ND.

	N Fines	Rock	Washed Dust	Dirty Dust	Lower Control Pt	Upper Control Pt
Sieve Size	% Passing	% Passing	% Passing	% Passing	% Passing	% Passing
5/8" (16mm)	100	100	100	100	100	100
1/2" (12.5mm)	100	92	100	100	90	100
3/8" (9.5mm)	99	62	100	100		
#4 (4.75mm)	83	3	86	93		
#8 (2.36mm)	65	1	45	68	28	58
#16 (1.18mm)	45	1	26	47		
#30 (0.6mm)	23	1	14	33		
#50 (0.3mm)	8	1	7	23		
#100(0.15m m)	6	1	4	16		
#200(0.075m m)	4.5	1	2.1	12.7	2	7
Pan	0	0	0	0	0	0

Table 5: Mix design.

PG 58-28		PG 64-28	
Materials	Percent (%)	Materials	Percent (%)
Binder	6.1	Binder	5.4
Crushed Rock	38	Crushed Rock	24
Natural Fines	25	Natural Fines	12
Washed Dust	19	Washed Dust	41
Dirty Dust	18	Dirty Dust	23

### 3.8 HMA compaction

Superpave Gyratory Compactor (SGC) was used to make the HMA specimen by following ASTM D6925-15 (ASTM, 2015) standard procedure. The Gyratory Compactor used to prepare the sample is shown in Figure 11.



Figure 11: Superpave Gyratory Compactor.

The mix was first made in the laboratory using the percentage of materials stated in the mix design. All the aggregates were heated to 325°F and the asphalt binder was heated to 290°F. All other equipment used for mixing was heated enough in the oven before using to ensure the mixing temperature of 280°F. For each mix, a batch mix of 3100 gm was used. After mixing each batch mix was put into the oven for 2 hours to simulate the plant mixing and placing in the field conditions. After 2 hours, a pre-weighted amount of mix was poured into the mold and compacted it in SGC. How much of weight of mix to be used to make the sample is also a trial and error process. The weight of the mix was adjusted

to standard air void content in the sample that was  $7\pm 1\%$ . Compaction pressure and angle were maintained to  $600\pm 60\text{kPa}$  and  $1.25\pm 0.02^\circ$ , respectively. This angle during compaction was used to simulate the vehicle-tire interaction in the field.

### **3.9 Rutting Resistance Test by APA**

Asphalt Pavement Analyzer (APA) developed by Strategic Highway Research Program (SHRP) is commonly used for evaluating rutting resistance of HMA sample. It is a standard test selected for its fastness, cost-effectiveness, and practicability (Suleiman and Mandal, 2013). The APA machine used for the test is shown in Figure 12.



Figure12: APA machine test chamber.

This test method simulates the traffic loading and temperature effects on compacted mixtures in the laboratory. This test simulates the traffic loading and temperature effects on compacted mixtures. The test was conducted in accordance with AASHTO TP 63-03 “Standard Method of Test for Determining Rutting Susceptibility of Asphalt Paving Mixtures” (AASHTO 2003). Two specimens of each type of dry conditioned were used for the test. Testing temperature was used based on the mixture virgin binder’s performance grade. For the mixes of Highway-32, the temperature was maintained at 58°C inside the testing chamber while for the mixes of I-29, it was maintained at 64°C. Prior to APA testing, all the specimens were heated to high-performance grade temperature for 6 hours. Six specimens of each type were tested at a time. The load was applied to the specimen by a steel wheel which was resting on a pneumatic hose pressurized to 100 psi for 8000 cycles (Skok, 2002). Rutting depth on specimens created by the wheel was recorded automatically in the machine. Average values of 8 to 9 mm (0.31 to 0.35 in) ranges may be used as a performance limiting criteria at 8000 cycles for gyratory samples (Choubane et al., 2000). The 8000 cycles represent about 1 million “Rutting Equivalent Standard Axle Loads” (ESALs) which represents about 3 million total ESALs in Minnesota (Skok et al., 2002). APA performance specification for North Dakota highways is an average of 7mm rut depth for traffic levels of 0.3 to <3 million design ESALs (Suleiman, 2008). In this study, 7mm rut depth was accepted for the limiting criteria.

### **3.10 Low-temperature Cracking Resistance Test by DCT**

Two cylindrical specimens of each type were used for the DCT test. The geometry of the specimen for this test was cylindrical with a diameter of 150mm and height of 50mm. The compacted specimens of 75 mm were cut (using a concrete saw) to the height of 50

mm for meeting the height requirement of DCT test. A crack mouth opening of 35mm was created on the specimen after creating a flat face in the specimen. Specific dimensions are shown in Figure 13 and test setup is shown in Figure 14.

Disc-Shaped Compact Tension (DCT) was carried out to analyze the low-temperature cracking resistance of the specimen. This test gives the fracture energy ( $G_f$ ), which is a parameter to describe the cracking resistance of the HMA specimen. The test was conducted in accordance with ASTM D7313 (ASTM 2013). The test was conducted at  $PG+10^{\circ}C$  of the low-temperature of the virgin binder used in the mixture. All the specimens were tested at  $-18^{\circ}C$ . Before testing, the specimens were conditioned for 12h at  $-18^{\circ}C$ . During the test, a constant Crack Mouth Opening Displacement (CMOD) rate of 0.017 mm/s was maintained.

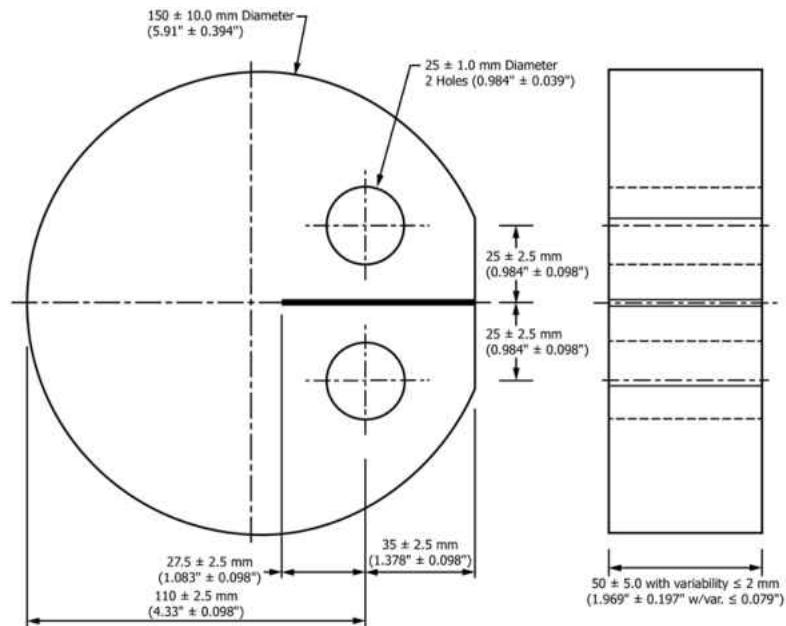


Figure 13: Dimension of DCT Specimen (ASTM 2013).

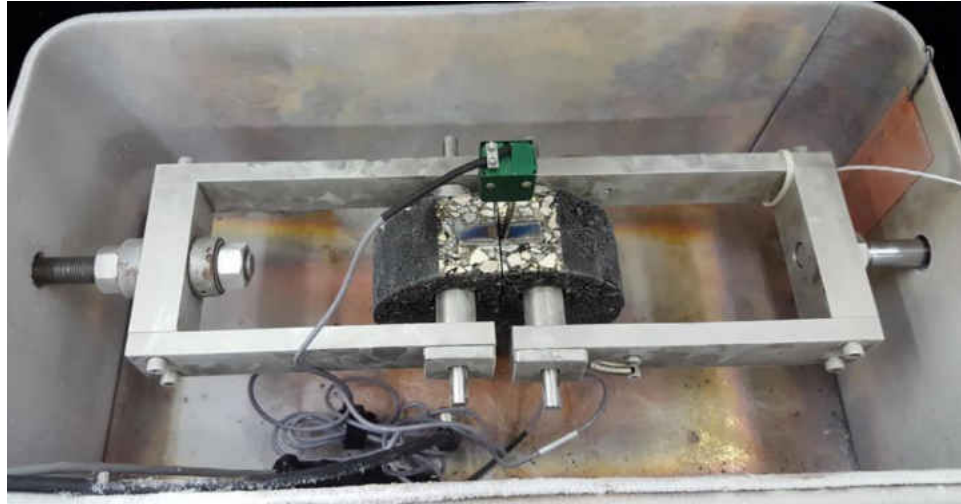


Figure 14: DCT test setup.

### 3.11 Fatigue Cracking Test by SCB

There are several standards for SCB test and researchers have been working to fine-tune the standards. Different states follow different geometry, notch depth, thickness, and temperature for the test. For this research, the Illinois-Flexibility Index Tester (I-FIT) protocol was followed. Recommended sample thickness for this test is 50mm like the DCT but with the limited materials available, the samples tested were at  $25\pm 2$  mm. The test specimen geometry details are shown in Figure 15 and test setup is shown in Figure 16. It's a semi-circular geometry with 150mm diameter and a notch of 15 mm was prefabricated in the flat end of the semi-circle. The testing temperature was set to  $25^{\circ}\text{C}$  recommended by I-FIT and the samples were conditioned in the environmental chamber for  $2\pm 0.2$  hrs. The test was run and post processed for calculating the fracture energy and Flexibility Index (FI) using a software. A preloaded force of 0.1kN was applied and the test applied load line displacement control at a rate of 50 mm/min. The higher the FI value the better the mix in terms of cracking resistance (ductility). For good performing mix, FI value is greater than 4.5 where less than 2 referred the very poor mix (Ozer et al., 2016).



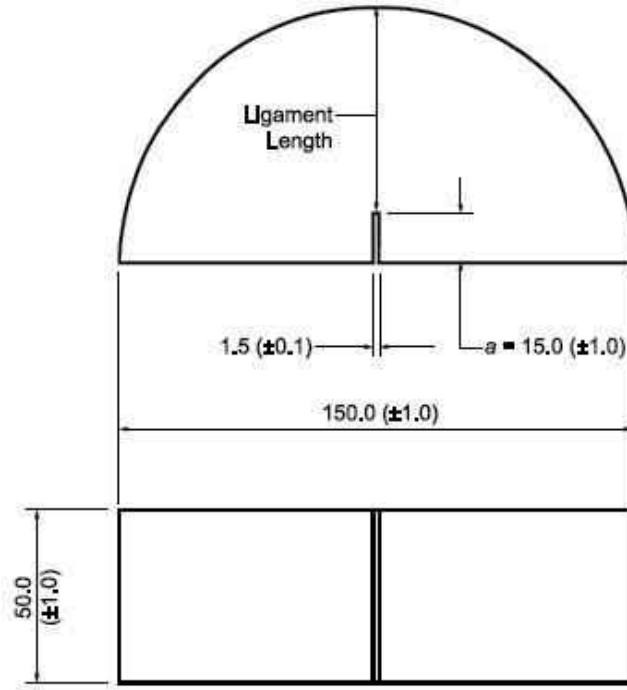


Figure 15: SCB test specimen Geometry (AASHTO, 2016).



Figure 16: SCB test setup.

### 3.12 Data Analysis

All the data collected from the different tests were analyzed to conclude the results of this study. Performance properties of the binder and mix were inferred from the result obtained from data analysis. Binders' test data were analyzed to see the rheological

properties of the binder. The analysis was done in two ways. First, the test result was compared to the standard threshold value specified by the different standards like ASTM, AASHTO etc. In addition to that, the test results were compared with the control specimen results' graphically to assess the convergence and divergence of the properties of modified specimens.

For the mixes, data from separate tests were analyzed separately using graphical images and statistical analysis. Control specimen and specified standard values were also used to infer the results of the study. Average of APA rut data for four different passes (2000, 4000, 6000, & 8000) were calculated for both control and study samples and compared it with the specified value. Graphical images were drawn to show the variation of the results with control specimen. Progression of rut depth with the passes was also delineated in the graph.

DCT and SCB data were analyzed in both graphically and statistically to measure performance and the significance of the results. Collected SCB data from the test were first analyzed with the post processing software that came up with the machine. Fracture energy and I-FIT index were calculated from the software. Average, standard deviation and coefficient of variation of the results were then calculated. Similarly, DCT fracture energy test data were also analyzed with the software during the test. Finally, independent t-test was done to see the statistical significance of the results. All the results from binder and mixture tests are shown in Chapter IV.

## **CHAPTER IV**

### **RESULTS AND DISCUSSIONS**

#### **4.0 General**

The study was done to analyze the effect of bio-binder on both binder and HMA mix with high RAP. Rheological properties of the binder containing high RAP content and bio-binder were tested using DSR test. Rutting, fatigue cracking, and low-temperature cracking resistance of HMA were tested using APA, SCB, and DCT test respectively. Binder tests results and HMA mix tests results are discussed in two sections separately.

#### **4.1 Effect of Bio-binders on Binder Rheology**

Rheology is used to assess the performance of the binder. Asphalt binder is tested for finding rutting and fatigue performance. Rheology at low-temperature is also tested for analyzing the low-temperature cracking. Rutting is an early stage pavement distress, hence Superpave specification specifies to test the unaged and short-term aged binder sample for analyzing the rutting resistance of the binder. RTFO aged sample is the short-term aged sample which simulates the early stage pavement field condition. PAV aged sample simulates the long term aging of the binder in the field condition that is used to analyze the fatigue resistance of the binder specified by the Superpave specification. All types of binder, unaged, RTFO aged, and PAV aged are used to test the low-temperature cracking resistance.

#### 4.1.1 Rutting Resistance

DSR test on different types of binder provided the complex shear modulus ( $G^*$ ) and phase angle ( $\delta$ ). The elastic portion [ $G^*/\sin(\delta)$ ] of the viscoelastic binder should be higher at the corresponding PG high-temperature grade to resist the permanent deformation of the binder under wheel load during the early stage of the pavement life. Superpave specification limits the minimum value of the elastic portion. For the Unaged binder, [ $G^*/\sin(\delta)$ ] should be higher than or equal to 1000 Pa at any strain level. A higher value of [ $G^*/\sin(\delta)$ ] in different percentage of shear strain is termed stiffer binder and expected to resist the deformation.

Figures 17 and 18 show the Unaged binders complex shear modulus at different shear strain level at 58°C. From Figure 17, it is seen that 100% RAP binder is the stiffest among the binders. From Figure 18, it is observed that Virgin PG 58-28, and 5%SOY\_25%PG58-28\_70%RAP binders pass the critical value of 1000 Pa while 5%WCO\_25%PG58-28\_70%RAP, 15.5%SOY\_84.5%RAP, and 16.5%WCO\_83.5%RAP binders couldn't pass the critical value of 1000Pa. These three binders are softer than the virgin PG58-28 binder.

Figures 19 and 20 show the Unaged binders complex shear modulus at different shear strain level at 64°C. It is observed from Figure 19 that 100% RAP binder is the stiffest. From Figure 20, it is observed that three modified binders: 5%SOY\_25%PG64-28\_70%RAP, 5%WCO\_25%PG64-28\_70%RAP, and 5%WCO\_35% PG64-28\_60%RAP are softer than the virgin PG64-28 binder and couldn't pass the critical value as well. The addition of bio-oil softens the binder and makes the binder susceptible to rutting.

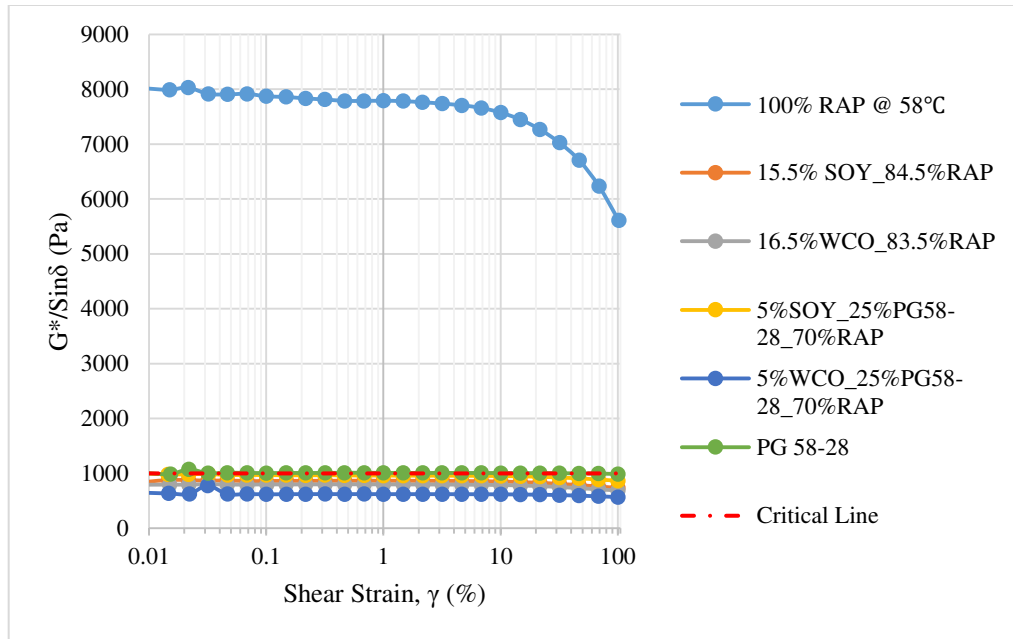


Figure 17: Unaged binders in different combination of bio-binder and RAP binder @ 58°C with 100% RAP binder.

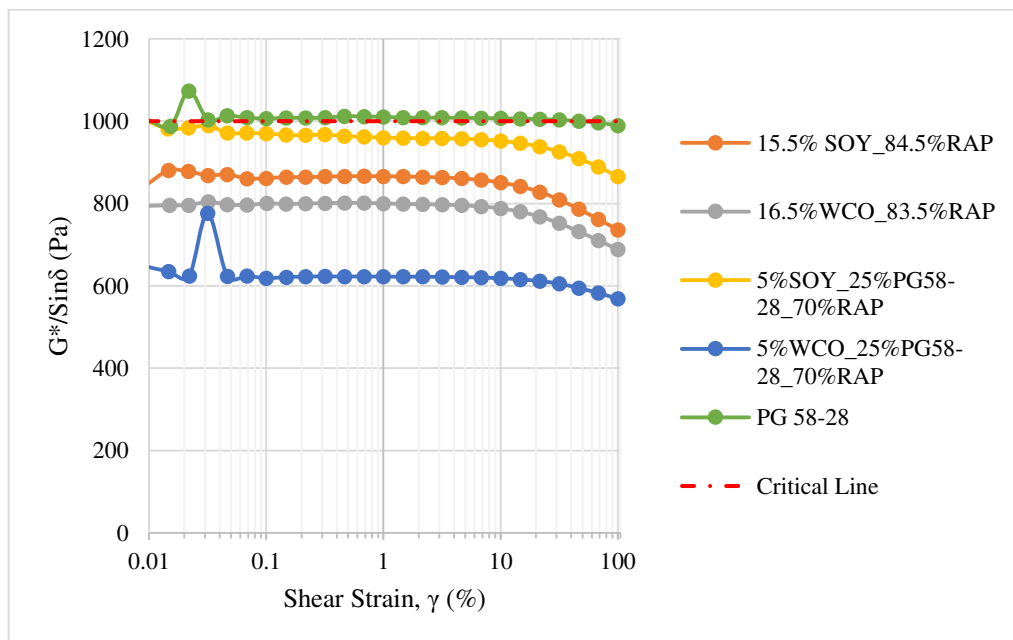


Figure 18: Unaged binders in different combination of bio-binder and RAP binder @ 58°C without 100% RAP binder.

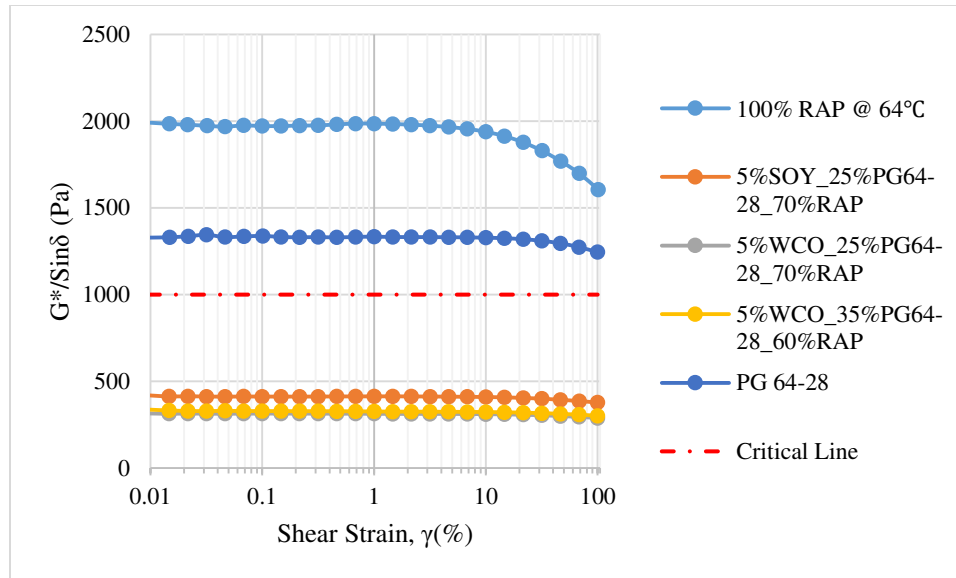


Figure 19: Unaged binders in different combination of bio-binder and RAP binder @ 64°C with 100% RAP binder.

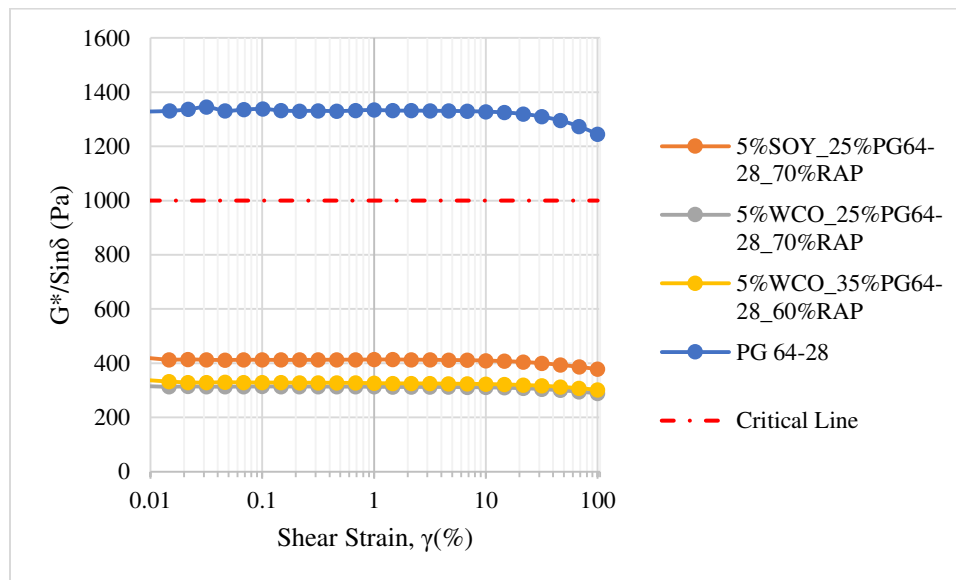


Figure 20: Unaged binders in different combination of bio-binder and RAP binder @ 64°C without 100% RAP binder.

For RTFO aged binder,  $[G^*/\sin(\delta)]$  should be higher than or equal to 2200 Pa at any strain level. A higher value of  $[G^*/\sin(\delta)]$  is expected to resist the deformation. Figures 21 and 22 show the RTFO aged binders complex shear modulus at different shear strain level at 58°C. 100% RAP binder is the stiffest as expected as observed from the Figure 21.

Figure 22 shows 5%SOY\_25%PG58-28\_70%RAP, and 5%WCO\_25%PG58-28\_70%RAP binders have the value near 8000Pa while Virgin PG58-28 barely passes the critical value of 2200Pa. The stiffness of PG58-28, 15.5% SOY\_84.5%RAP, and 16.5%WCO\_83.5%RAP binders are almost the same. Comparing the results between Figure 18 and Figure 22, it is observed that 5%SOY\_25%PG58-28\_70%RAP, and 5%WCO\_25%PG58-28\_70%RAP modified binders aged quickly as the results of Unaged and RTFO aged binder stiffness variation is significant. 5%SOY\_25%PG58-28\_70%RAP, and 5%WCO\_25%PG58-28\_70%RAP modified binders have better potential than virgin PG 58-28 to resist rutting.

Figures 23 and 24 show the RTFO aged binders complex shear modulus at different shear strain level at 64°C. All the binders pass the critical of 2200 Pa, which means they are good against rutting. 100%RAP is the stiffest binder as expected while 5%SOY\_25%PG64-28\_70%RAP is stiffer than the virgin PG64-28 binder. 5%WCO\_25%PG64-28\_70%RAP binder shows the same stiffness as of virgin PG64-28 binder. Modified binder with 60% RAP (5%WCO\_35% PG64-28\_60%RAP) shows the lowest stiffness and susceptibility to rutting is the highest. Though the Unaged modified binders (Figure 20) couldn't pass the critical value, all RTFO aged modified binder pass the critical value. Short-term RTFO aged binder property is critical for pavement design and for rutting susceptibility as compared to the unaged binder.

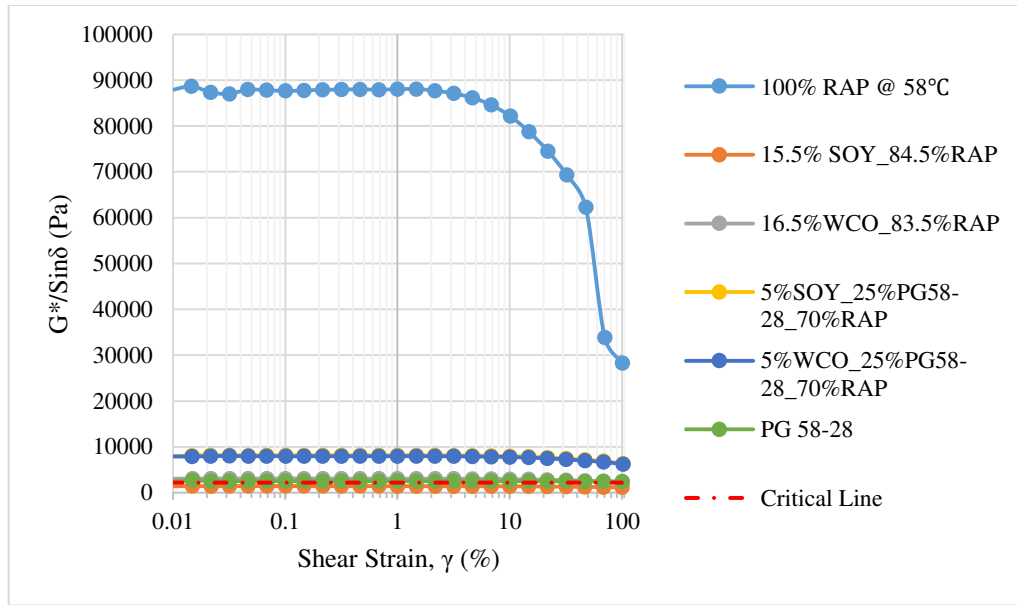


Figure 21: RTFO aged binders in different combination of bio-binder and RAP binder @ 58°C with 100% RAP binder.

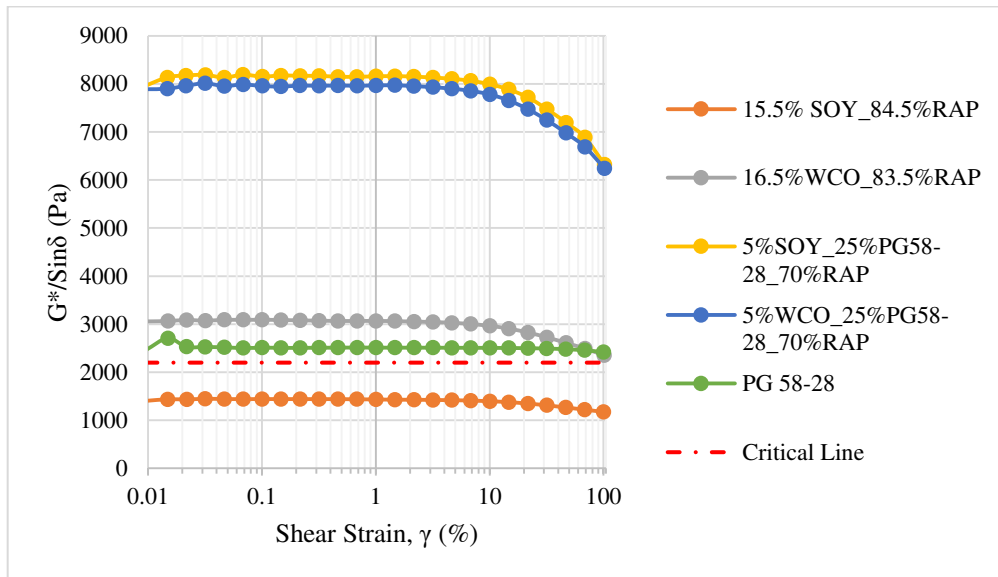


Figure 22: RTFO aged binders in different combination of bio-binder and RAP binder excluding 100% RAP binder @ 58°C without 100% RAP binder.



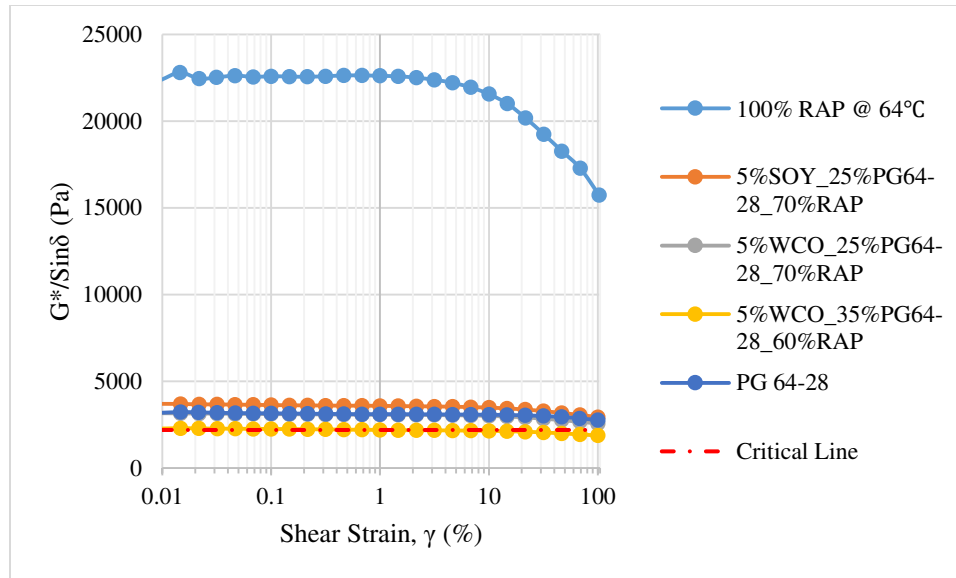


Figure 23: RTFO aged binders of different combination of bio-binder and RAP binder @ 64°C with 100% RAP binder.

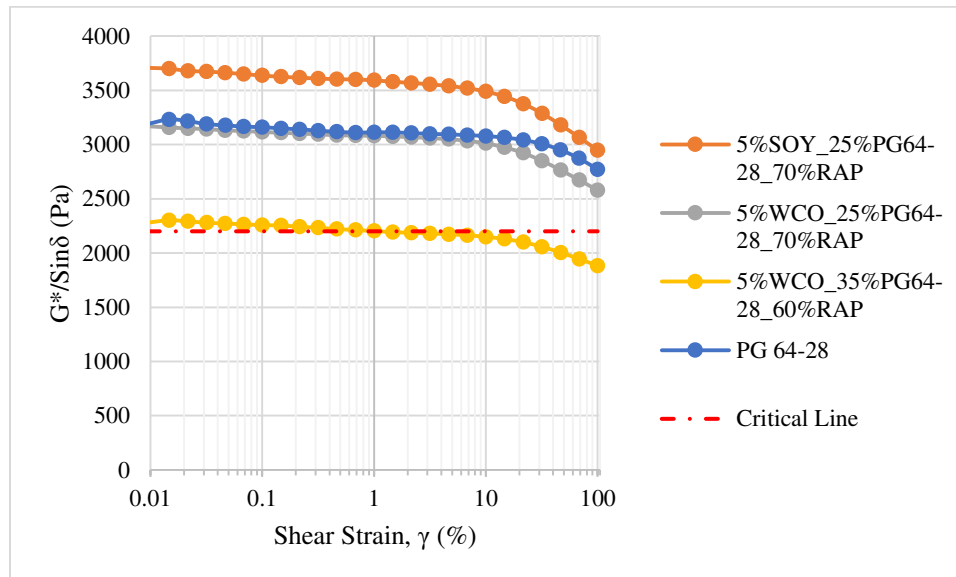


Figure 24: RTFO aged binders of different combination of bio-binder and RAP binder excluding 100% RAP binder @ 64°C without 100% RAP binder.

#### 4.1.2 Fatigue Resistance

Fatigue resistance is the long-term pavement performance during the service life of the pavement. To simulate this field condition PAV aged binder was used in the test. Asphalt binder should not be too stiff for resisting the fatigue cracking. That's why

Superpave specification limits the viscous portion  $[(G^*)\sin(\delta)]$  of the asphalt binder should be minimum under dynamic loading. The specified value should be lower than 5000 kPa in all applied shear strain level.

Figures 25 and 26 show the PAV aged binders complex shear modulus at different shear strain level at 58°C. It is observed from the Figure 25 that all the binders have a lower stiffness than the critical value of 5000 kPa. But 100% RAP binder shows the highest stiffness which makes the binder highly susceptible to fatigue cracking. Modified binder of 5%SOY\_25%PG58-28\_70%RAP and 5%WCO\_25%PG58-28\_70%RAP have almost the same value of stiffness but higher than the PG58-28 binder's stiffness as seen from the Figure 26. Two other modified binders, i.e., 15.5% SOY\_84.5%RAP, and 16.5%WCO\_83.5%RAP also possess higher stiffness than the stiffness of PG-58-28 but lower than the stiffness of 5%SOY\_25%PG58-28\_70%RAP, and 5%WCO\_25% PG58-28\_70%RAP binder which contain 25% virgin binder.

Figures 27 and 28 show the PAV aged binders complex shear modulus at different shear strain level at 64°C. All the binders are well below the critical value of 5000 kPa. 100% RAP binder shows the highest stiffness. Modified binder of 5%SOY\_25%PG64-28\_70%RAP and 5%WCO\_25%PG64-28\_70%RAP have the higher stiffness while another modified binder of 5%WCO\_35%PG64-28\_60%RAP has a lower stiffness than the stiffness of virgin PG64-28 binder. According to the test results, 5%WCO\_35%PG64-28\_60%RAP binder possess the highest fatigue-resistance property.

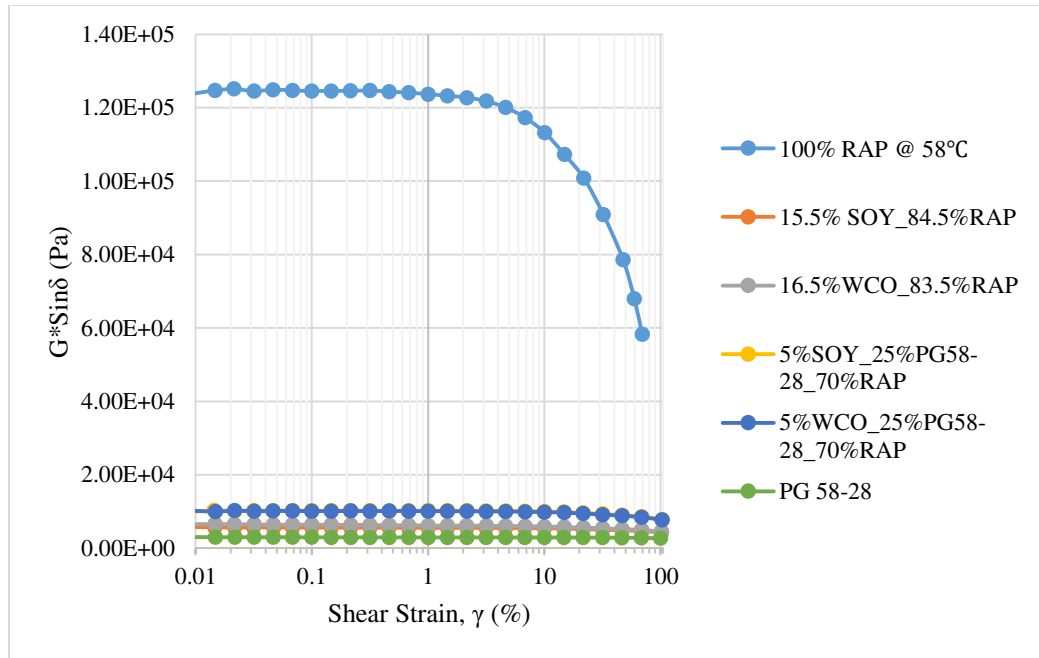


Figure 25: PAV aged binders in different combination of bio-binder and RAP binder @ 58°C with 100% RAP binder.

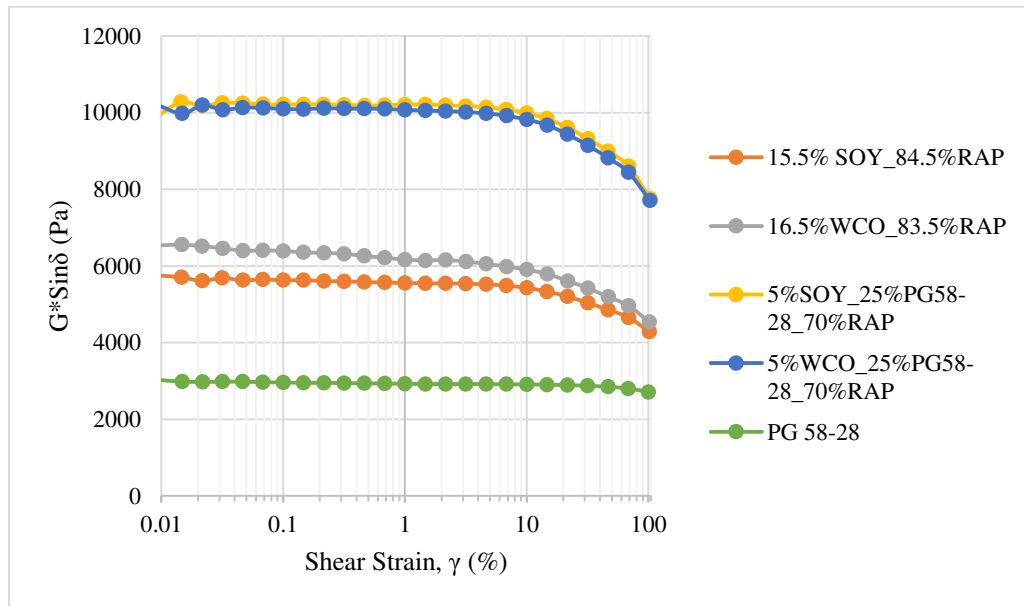


Figure 26: PAV aged binders of different combination of bio-binder and RAP binder @ 58°C without 100% RAP binder.

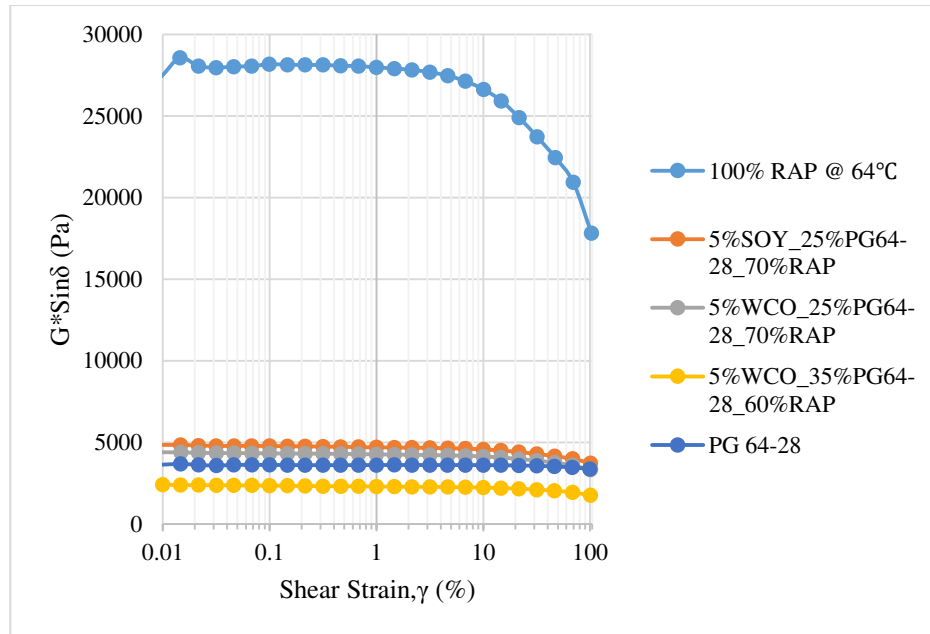


Figure 27: PAV aged binders of different combination of bio-binder and RAP binder @ 64°C with 100% RAP binder.

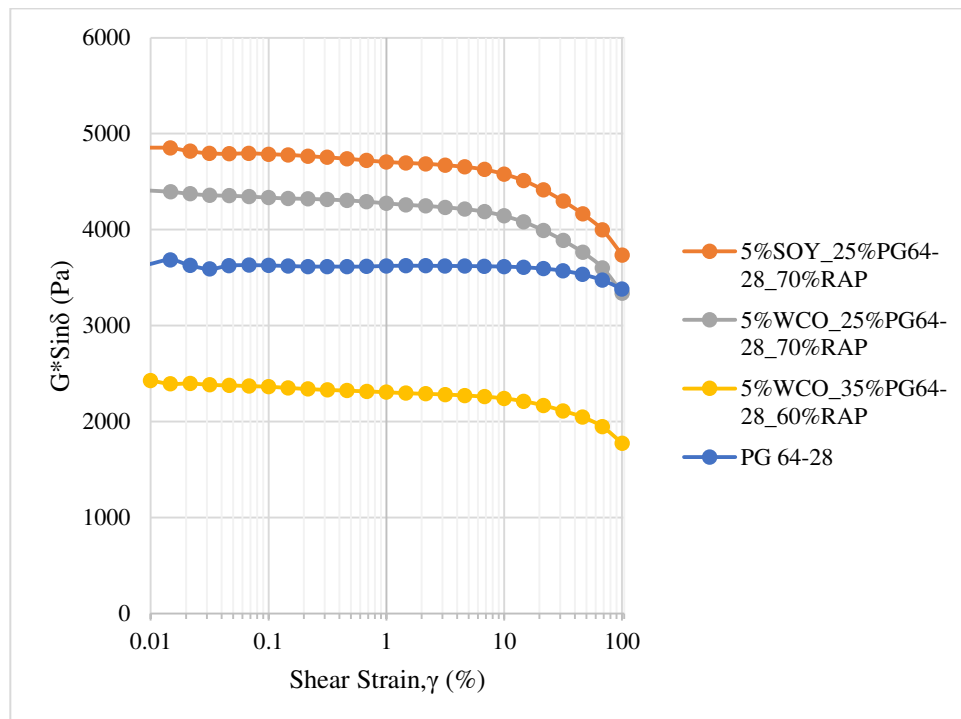


Figure 28: PAV aged binders in different combination of bio-binder and RAP binder @ 64°C without 100% RAP binder.

### 4.1.3 Low-Temperature Cracking Resistance

The low-temperature cracking resistance of the binder was tested using the DSR machine following the method published by Farrar et al., (2015). A master curve was generated at low-temperature PG+10°C from which relaxation modulus  $G(t)$  at 60 second and corresponding slope ( $m_r$ ) of the graph of  $\text{Log } G(t)$  vs.  $\text{Log (Reduced } t)$  was estimated. A series of steps were followed to estimate the  $m_r$  and  $G(t)$  values for each binder type. A 4mm diameter sample was used to do this test where two frequency sweeps were done at PG+10°C and PG+20°C. The frequency sweeps provided the storage modulus [ $G'(\omega)$ ] in all corresponding frequency ( $\omega$ ) values. Storage modulus [ $G'(\omega)$ ] vs frequency ( $\omega$ ) for both frequency sweeps are shown in Figure 29.

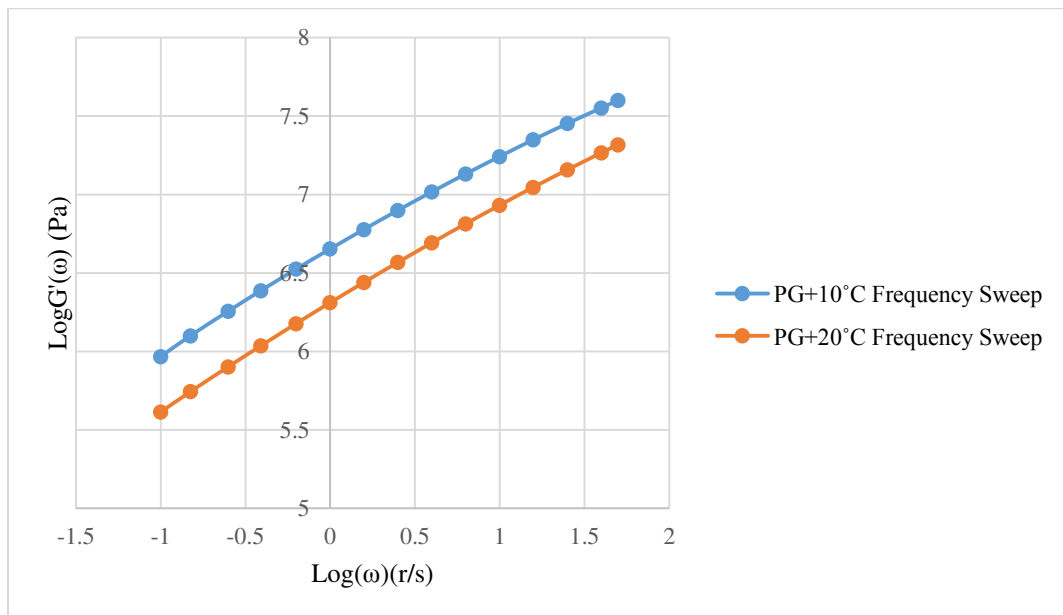


Figure 29: Sample graph of PG+10°C and PG+20°C frequency sweeps.

A horizontal shift factor,  $a_T$  was then calculated to shift the PG+20°C frequency sweep along the abscissa to overlap with the PG+10°C frequency sweep by time-temperature superposition (TTS). The resultant graph after the superposition is known as

the master curve of storage modulus [ $G'(\omega)$ ] at low-temperature PG+10°C which is shown in Figure 30.

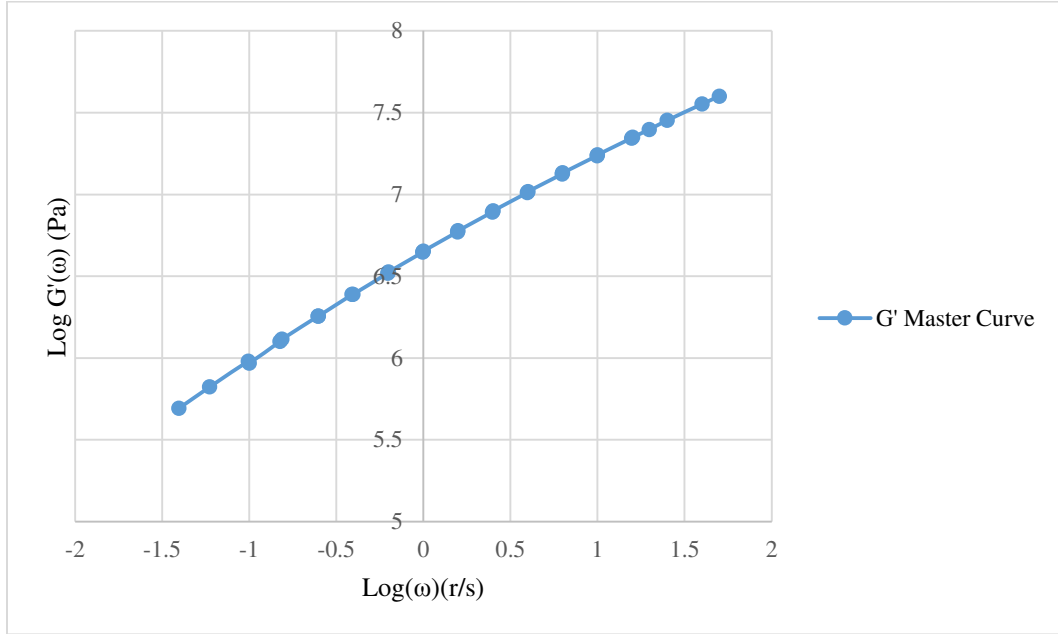


Figure 30: Sample graph of  $G'(\omega)$  Master curve at a reference temperature of PG+10°C.

An approximation method developed by Christensen (2012) for viscoelastic materials was then used to estimate the relaxation modulus  $G(t)$  (Christensen, 2012). In the method, for viscoelastic materials, the approximated expression is shown in Eq.(4.1).

$$G(t) \approx G'(\omega)|_{\omega=2\pi/t} \dots \dots \dots \text{Eq.(4.1)}$$

Using this expression, a graph of Log [ $G(t)$ ] vs. Log (Reduced t) was constructed which is shown in Figure 31.

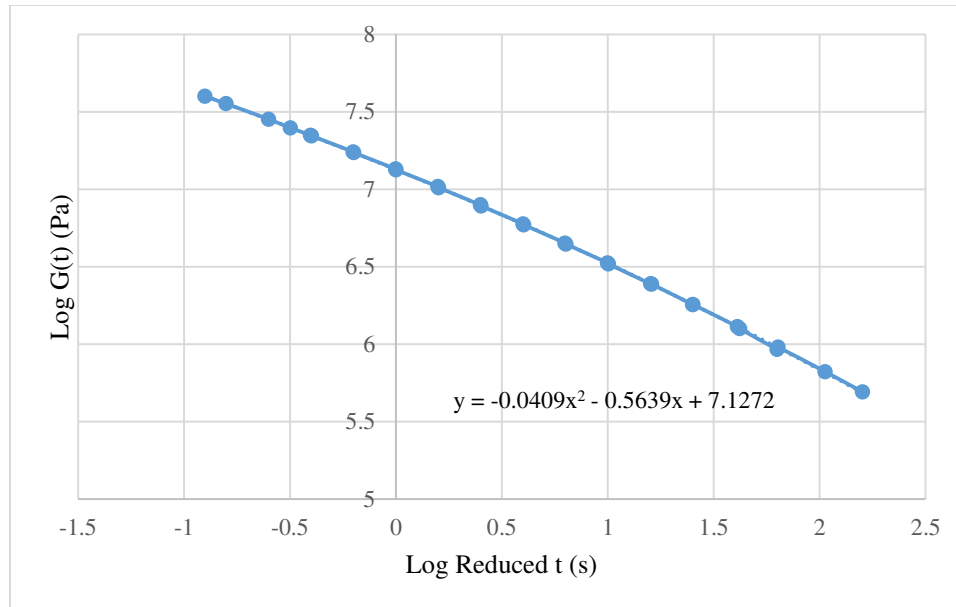


Figure 31: Relaxation modulus master curve to determine  $m_r$  (60s) and  $G(60s)$ .

Finally, a 2<sup>nd</sup> polynomial was fitted to the graph for getting the equation of the graph. The slope ( $m_r$ ) of the graph at 60 second was then estimated from the 1<sup>st</sup> order derivative of the equation. A solution of this equation provided the relaxation modulus [ $G(t)$ ] at 60 seconds which is also known as creep stiffness of the binder.

All these steps mentioned above were followed to estimate the  $m_r$  &  $G(t)$  values at 60 seconds for each binder sample type. The summary results of  $G(60s)$  and  $m_r$  value are shown in Tables 6 and 7 respectively. All the creep stiffness &  $m_r$  values were compared with the AASHTO M320 specified values and with virgin binder test values. AASHTO M320 specifies a maximum creep stiffness value (300MPa) since a higher creep stiffness value indicates higher thermal stresses i.e. lower low-temperature cracking resistance. It also specifies a minimum  $m_r$ -value (0.300) since a lower  $m$ -value indicates a lesser ability to relax stresses which make the binder prone to low-temperature cracking. Relaxation modulus and slope ( $m_r$ ) of different binders at three different aging conditions (i.e., Unaged, RTFO aged, and PAV aged) are plotted in bar graphs and are shown in Figure 32

to Figure 37. From the Figures 32, 33, and 34, it is observed that all the binders' relaxation modulus at low-temperature are below the 300MPa that satisfy the Superpave binder specification. Only for PAV aged 100% RAP binder, DSR machine couldn't do the time-temperature superposition for the frequency sweeps (-18°C frequency sweep, and -8°C frequency sweep).

From Figure 35 to Figure 37, it is observed that slope ( $m_r$ ) is the lowest for the RAP binder for both Unaged and RTFO aged type whereas for PAV aged RAP binder DSR machine couldn't do the time-temperature superposition for the frequency sweeps (-18°C frequency sweep, & -8°C frequency sweep). For modified and virgin binder  $m_r$  is above the Superpave specified value of 0.3 for all aged type binder. Hence, based on the obtained results, modified binder are expected to perform better against low-temperature cracking. Furthermore, for PAV aged modified binder of 5%SOY\_25%PG64-28\_70%RAP, and 5%WCO\_25%PG64-28\_70%RAP perform better than the PAV aged virgin PG58-28, and PG64-28 binder against low-temperature cracking.

Table 6: Relaxation modulus [G(60s)] in MPa for different types of binder with high RAP and bio-binder.

<b>Binder Type</b>	<b>Unaged</b>	<b>RTFO-Aged</b>	<b>PAV-Aged</b>
PG 58-28	6	5	11
5%SOY_25% PG58-28_70%RAP	1	5	7
5%WCO_25% PG58-28_70%RAP	6	5	8
PG 64-28	6	18	17
5%SOY_25% PG64-28_70%RAP	1	5	2
5%WCO_25% PG64-28_70%RAP	1	4	6
100% RAP	3	28	Can't Calc



Table 7: Slope ( $m_r$ ) of Relaxation modulus [G(60s)] for different types of binder with high RAP and bio-binder.

Binder Type	Unaged	RTFO-Aged	PAV-Aged
PG 58-28	0.7	0.6	0.5
5%SOY_25% PG58-28_70%RAP	0.7	0.6	0.5
5%WCO_25% PG58-28_70%RAP	0.7	0.6	0.5
PG 64-28	0.7	0.6	0.5
5%SOY_25% PG64-28_70%RAP	0.7	0.6	0.6
5%WCO_25% PG64-28_70%RAP	0.7	0.6	0.6
100% RAP	0.6	0.4	Can't Calc

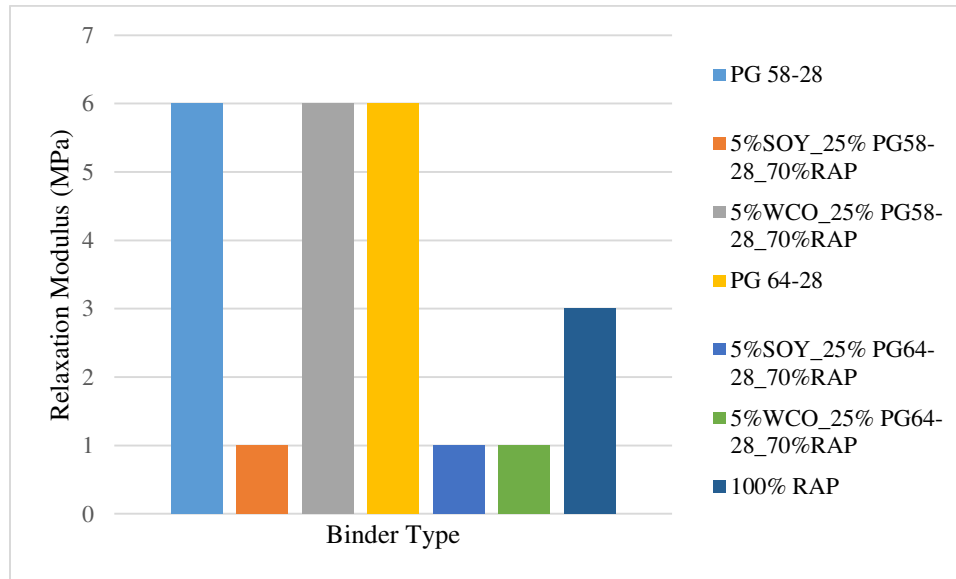


Figure 32: Relaxation modulus [G(60s)] for Unaged binder with high RAP and bio-binder.

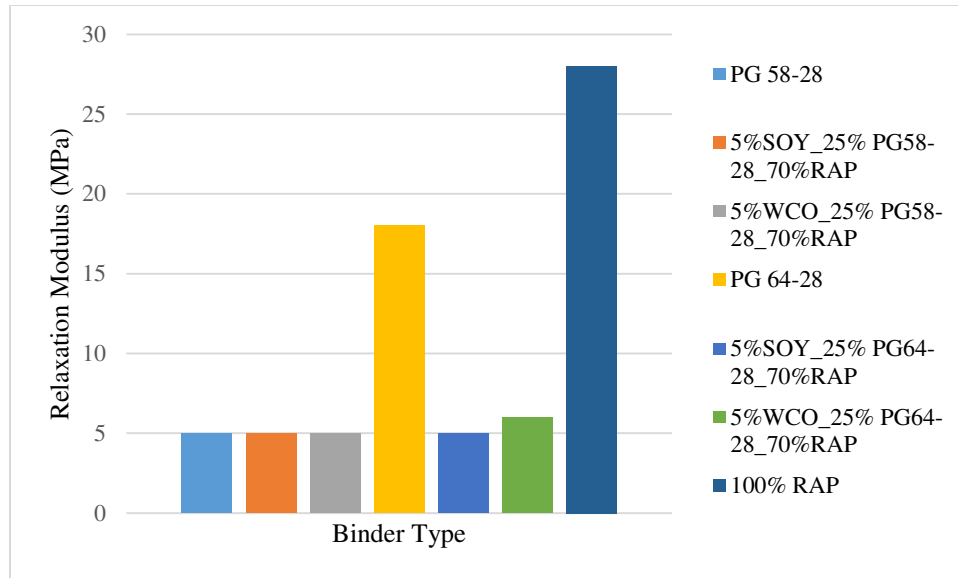


Figure 33: Relaxation modulus [G(60s)] for RTFO aged binder with high RAP and bio-binder.

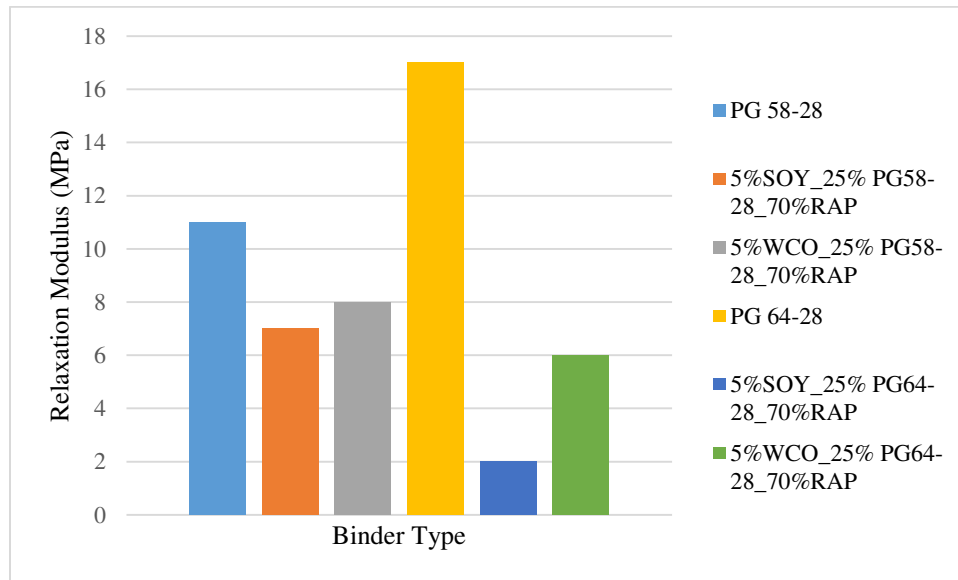


Figure 34: Relaxation modulus [G(60s)] for PAV aged binder with high RAP and bio-binder.

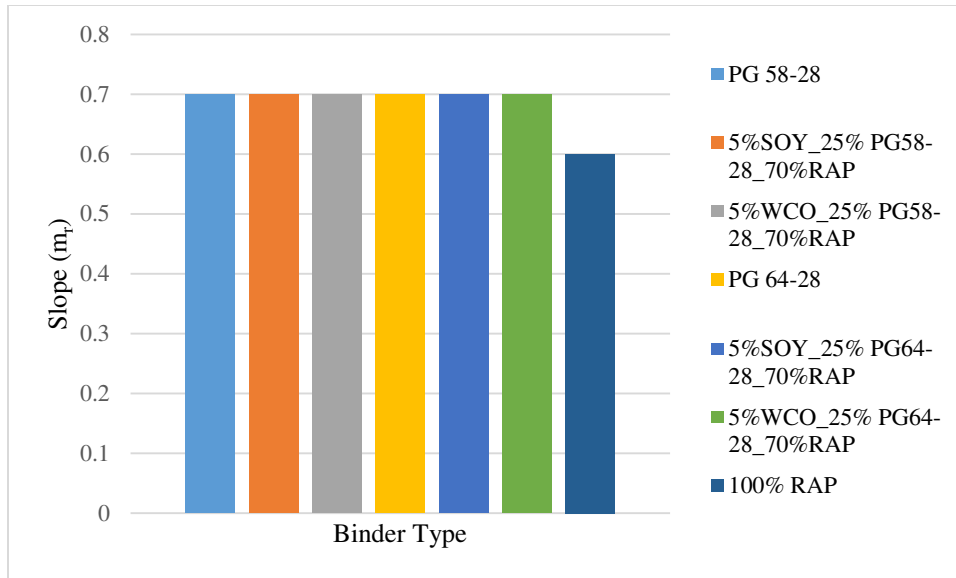


Figure 35: Slope ( $m_r$ ) for Unaged binder with high RAP and bio-binder.

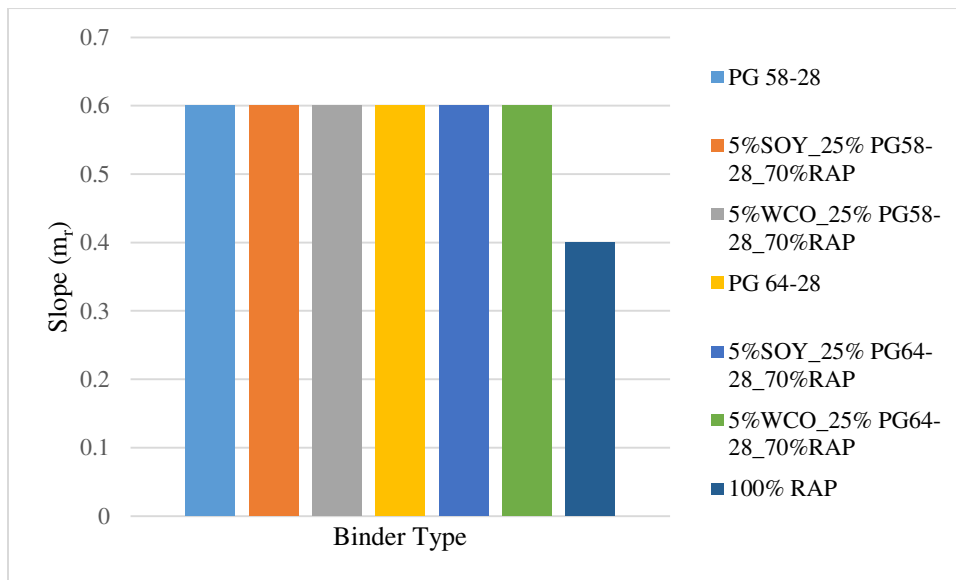


Figure 36: Slope ( $m_r$ ) for RTFO aged binder with high RAP and bio-binder.

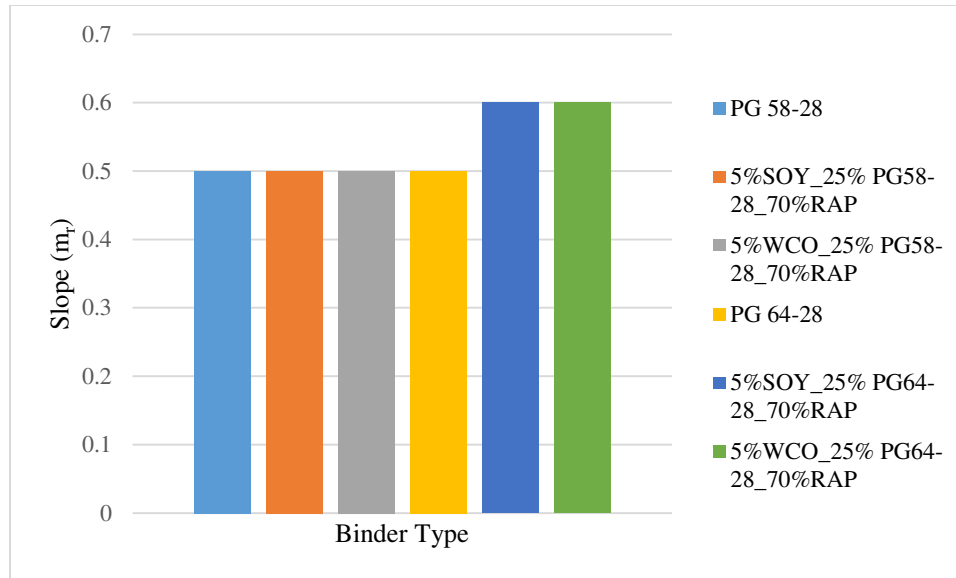


Figure 37: Slope ( $m_r$ ) for PAV aged binder with high RAP and bio-binder.

## 4.2 Effect of Bio-binders on HMA Mix

After performing the rheology tests of binders, the combination of binders were used to make the HMA specimens to assess the effects of bio-binder with high RAP binder on the performance of HMA specimen. Type of mixes is named according to the binder combinations used to make the mixes. Two different types of aggregates, collected from two different sites in North Dakota, were used to prepare the HMA specimen in the laboratory. Due to a shortage of aggregates and extracted binder all types of specimens couldn't be prepared. These constraints also limit the number of specimens that was prepared. However, all the prepared specimens were analyzed to assess three important performance properties. In the following three sections, the properties are discussed.

### 4.2.1 Rutting Resistance

Rutting resistance potential of the HMA mixes with different binder combinations was tested by performing the APA test. Two different temperatures were used for conducting the tests to conform to AASHTO T 340 standard. The specimens which were

prepared with Highway-32 materials and base binder of PG 58-28 were tested at 58°C while the specimens which were prepared with I-29 materials and base binder of PG-64-28 were tested at 64°C. Table 8 shows the results tested at 58°C and Table 9 shows the results tested at 64°C. A lower rutting depth is expected for delineating high rutting resistance potential of HMA. From both the tables it is seen that rut depth for all specimen is below the limiting performance criteria used in this study. The observed maximum rut depth for 5%WCO\_25%PG64-28\_70%RAP specimen at 64°C is 5.68mm while the limiting criteria is 7mm for this study. Average rut depths for different passes of different binder combinations at 58°C & 64°C are shown in Figure 38 and 39 respectively. 100% RAP binder shows the highest rutting resistance at all passes as expected because it is the stiffest binder. 5%SOY\_25%PG64-28\_70%RAP mix shows lower rut depth while 5%WCO\_25%PG64-28\_70%RAP shows higher rut depth than the PG 64-28 mix rut depth at 64°C. High RAP binder mix modified by only bio-binder (i.e., 15.5%SOY\_84.5%RAP, & 16.5% WCO\_83.5%RAP) performs well against rutting while tested at 58°C.

Table 8: APA Results Summary @ 58°C.

Mix Type	2000			4000			6000			8000		
	Avg. (mm)	St.D.	COV (%)	Avg. (mm)	St.D.	COV (%)	Avg. (mm)	St.D.	COV (%)	Avg. (mm)	St.D.	COV (%)
<b>PG 58-28</b>	1.38	0.27	19.66	1.75	0.28	15.77	1.89	0.22	11.82	2.04	0.16	7.64
<b>15.5% SOY_84.5% RAP</b>	1.73	0.20	11.49	1.90	0.09	4.50	2.05	0.09	4.51	2.11	0.08	3.63
<b>16.5% WCO_83.5% RAP</b>	2.21	0.06	2.90	2.68	0.03	1.21	2.90	0.03	0.90	3.00	0.04	1.22

Table 9: APA Results Summary @64°C.

Mix Type	2000			4000			6000			8000		
	Avg. (mm)	St. D.	COV (%)	Avg. (mm)	St.D.	COV (%)	Avg. (mm)	St. D.	COV (%)	Avg. (mm)	St.D.	COV (%)
<b>PG 64-28</b>	3.18	0.49	15.54	4.06	0.77	18.96	4.64	0.81	17.41	5.18	1.10	21.22
<b>100% RAP</b>	2.74	0.14	5.00	4.54	0.27	6.00	4.87	0.19	3.97	4.93	0.13	2.66
<b>5% WCO_25% PG 64-28_70% RAP</b>	4.14	0.19	4.68	5.03	0.16	3.18	5.49	0.33	5.99	5.68	0.08	1.32
<b>5% SOY_25% PG 64-28_70% RAP</b>	3.02	0.35	11.72	3.62	0.17	4.75	4.12	0.17	4.05	4.53	0.11	2.32

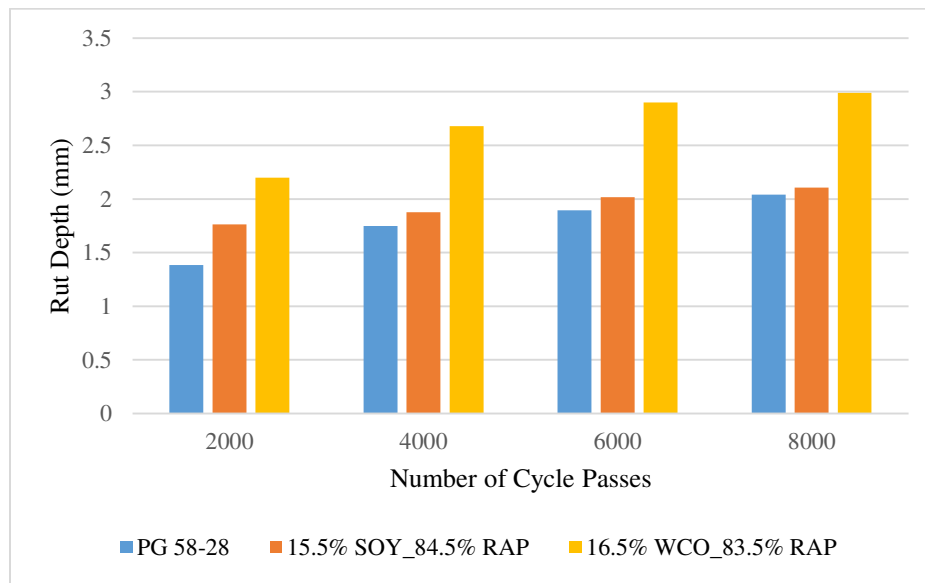


Figure 38: Average Rut Depth for different binder combinations with bio-binder and high RAP binder at 58°C.

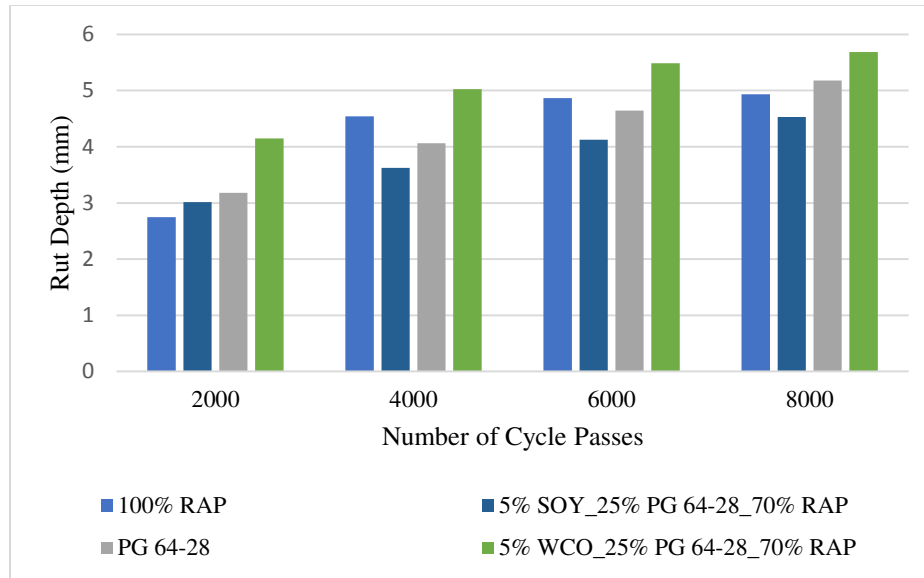


Figure 39: Average Rut Depth for different binder combinations with bio-binder and high RAP binder at 64°C.

To see whether there is any significant difference between the mixes or not an independent t-test was performed on the rutting test results. The test was done at 0.05 significance level. The test results of the mixes tested at 58°C and mixes tested at 64°C are shown in Table 10 and 11 respectively. In the table, ‘Y’ indicates that there is a significant difference and ‘N’ indicates there is no significant difference between the mixes performance. From Table 10, it is observed that PG 58-28 mixes don’t have a significant difference with modified mixes of 15.5%SOY\_84.5% RAP while having significant difference with modified mixes of 16.5% WCO\_83.5%RAP. Although two modified mixes don’t have any significant difference. From Table 11, it is observed that PG 64-28 mixes have significant difference with both the modified mixes of 5%WCO\_25%PG64-28\_70%RAP and 5%SOY\_25%PG64-28\_70%RAP and 100%RAP mixes as well. While both the modified mixes don’t have any significant difference. The tests results are not inclusive due to low sample size.

Table 10. APA Independent T-Test Summary for PG58-28 mixes.

Mix Type	PG 58-28	15.5% SOY_84.5% RAP	16.5% WCO_83.5% RAP
PG 58-28	X	Y	N
15.5% SOY_84.5% RAP	X	X	N
16.5% WCO_83.5% RAP	X	X	X

Table 11. APA Independent T-Test Summary for PG64-28 mixes.

Mix Type	PG 64-28	5% WCO_25% PG 64-28 _70% RAP	5% SOY_25% PG 64-28 _70% RAP	100% RAP
PG 64-28	X	Y	Y	Y
5% WCO_25% PG 64-28 _70% RAP	X	X	N	N
5% SOY_25% PG 64-28 _70% RAP	X	X	X	N
100% RAP	X	X	X	X

Air void content of the specimens tested for rutting resistance was drawn against rut depth to see the relationship between these two parameters. Figure 40 shows the specimens air void vs rut depth tested at 58°C and Figure 41 shows the specimens air void vs rut depth tested at 64°C. In both cases, the trend line was drawn. However, no correlation was observed between air void content and rut depth for these type of mixes.



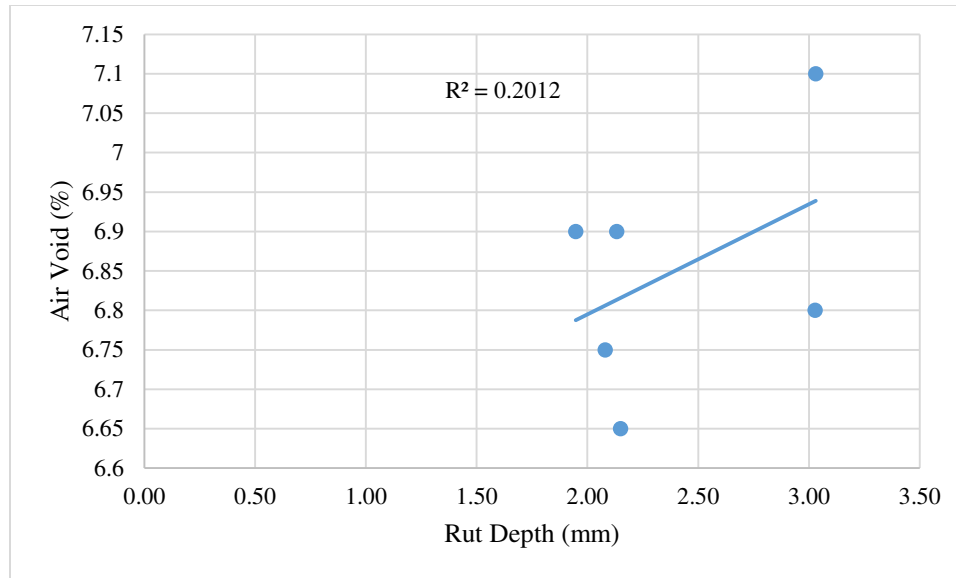


Figure 40: Air void vs rut depth of the specimens tested at 58°C.

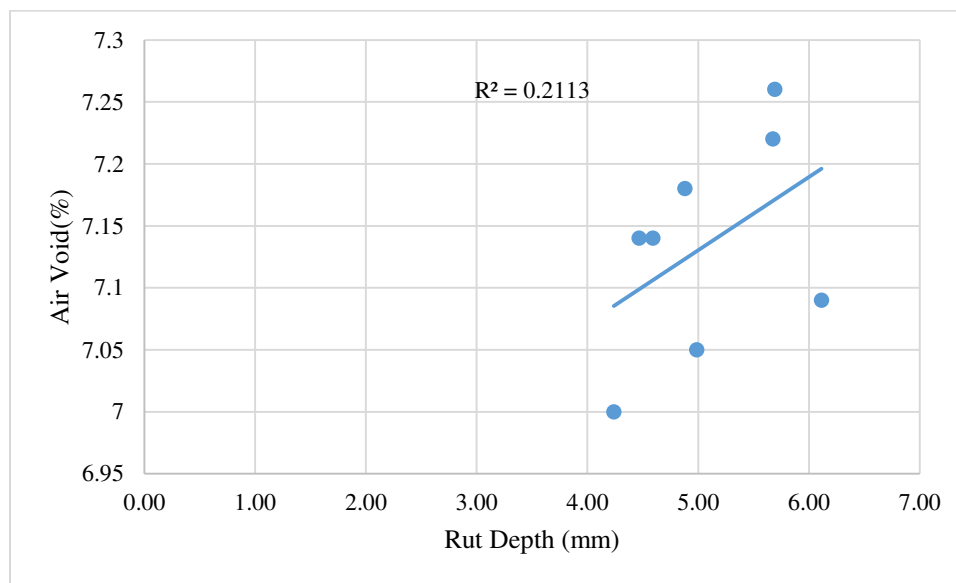


Figure 41: Air void vs rut depth of the specimens tested at 64°C.

#### 4.2.2 Fatigue Cracking Resistance

Resistance to fatigue cracking of HMA mix specimen was analyzed by performing the SCB test. SCB test on specimens was done at 25°C on the samples of 25mm thickness following the I-FIT prescribed test method. Though the specified thickness in the method was 50mm, due to limited availability of materials, all the tests were performed using

25mm thick specimens. In the test, two parameters were computed: fracture energy ( $G_f$ ), and flexibility index (FI). Two sample load-displacement graphs of calculating fracture energy and FI index found in SCB test are shown in Figures 42 and 43. A higher fracture energy and higher FI index are expected for HMA to perform better against fatigue cracking. Average fracture energy and FI index calculated from I-FIT of different mix types are shown in Table 12.

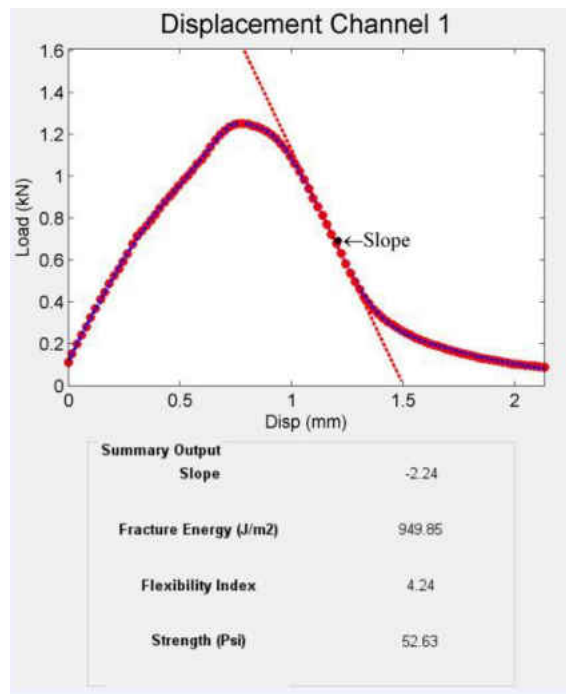


Figure 42: Sample load-displacement curve.

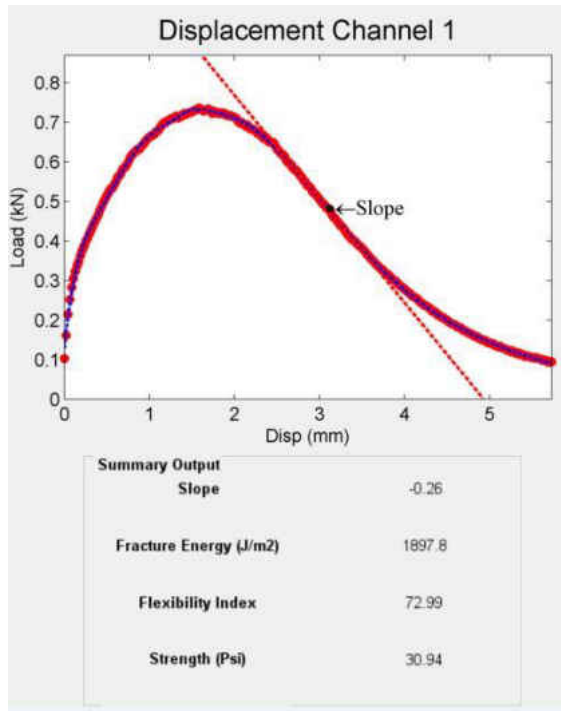


Figure 43: Sample load-displacement curve.

Table 12: Fracture Energies from SCB test.

Mix type	Average	
	Fracture Energy(J/m <sup>2</sup> )	FI
PG 58-28, Hwy 32	942.08	4.11
PG 64-28, I-29	1540.77	57.37
5%SOY_25%PG64-28_70%RAP(I-29)	1073.81	14.90
5%WCO_25%PG64-28_70%RAP(I-29)	1072.66	16.23
100% RAP (I-29)	1245.53	1.59
100% RAP (Hwy-32)	418.53	0.36
15.5% SOY_84.5% RAP (Hwy-32)	480.47	0.65
16.5% WCO_83.5% RAP (Hwy-32)	407.99	0.57

Average fracture energy of different types of mixtures is plotted in the graph and is shown in Figure 44 while FI indexes are plotted in the graph and is shown in Figure 45. HMA mix with a virgin binder of PG 64-28 appears to be the most fatigue resistant among the mixes as it showed the highest fracture energy as well as the highest FI index. Mixes with binder 5%SOY\_25%PG64-28\_70%RAP(I-29) and 5%WCO\_25%PG64-

28\_70%RAP(I-29) have shown approximately 30% less energy than the energy of the mixture of PG 64-28 binder. Though FI indexes of these two mixes are also less than the PG 64-28 mixes, these are well above 4.5 and according to I-FIT criteria, it is a good performing mix. But surprisingly 100% RAP (I-29) mixes are shown higher energy than the energy of these two mixes. However, FI index of 100% RAP is less than 2.0 and according to I-FIT, it is a poor mix and susceptible to fatigue cracking. Mixtures 15.5% SOY\_84.5% RAP (Hwy-32) and 16.5% WCO\_83.5% RAP (Hwy-32) (without virgin binder) have shown 50% less energy than the mixes with 100% PG 58-28 binder. The FI indexes of these two mixes are also below 1.0 that can be termed as a very poor mix. It is observed because probably only bio-binder couldn't fully rejuvenate the high percentages of RAP binder in the mix.

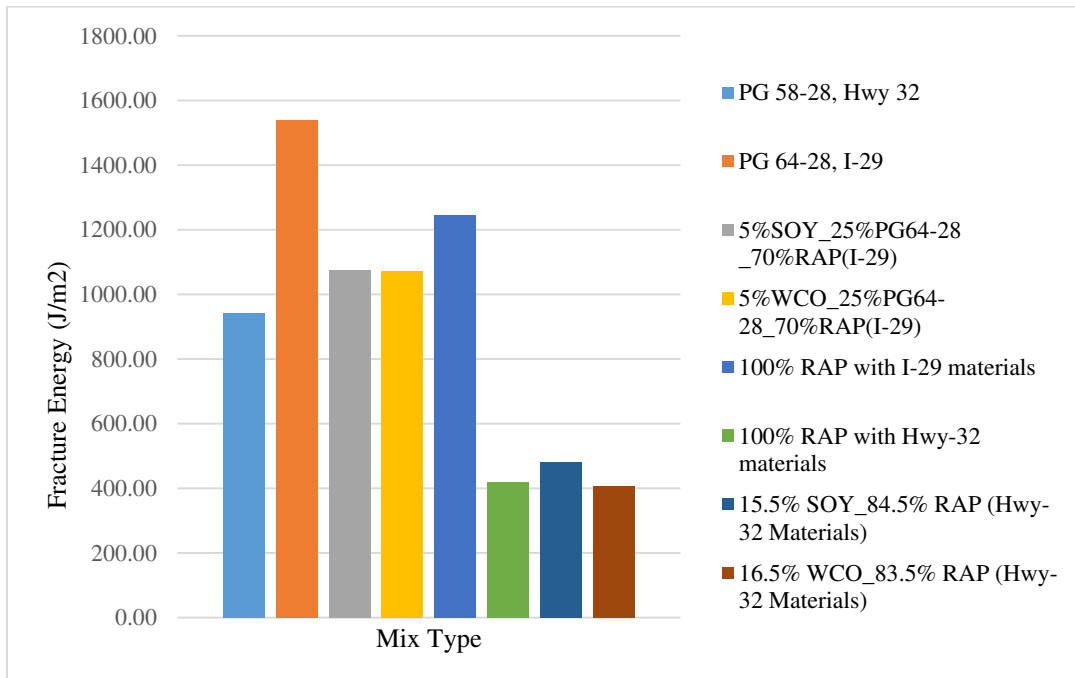


Figure 44: Average Fracture Energies of different types of HMA mixes.

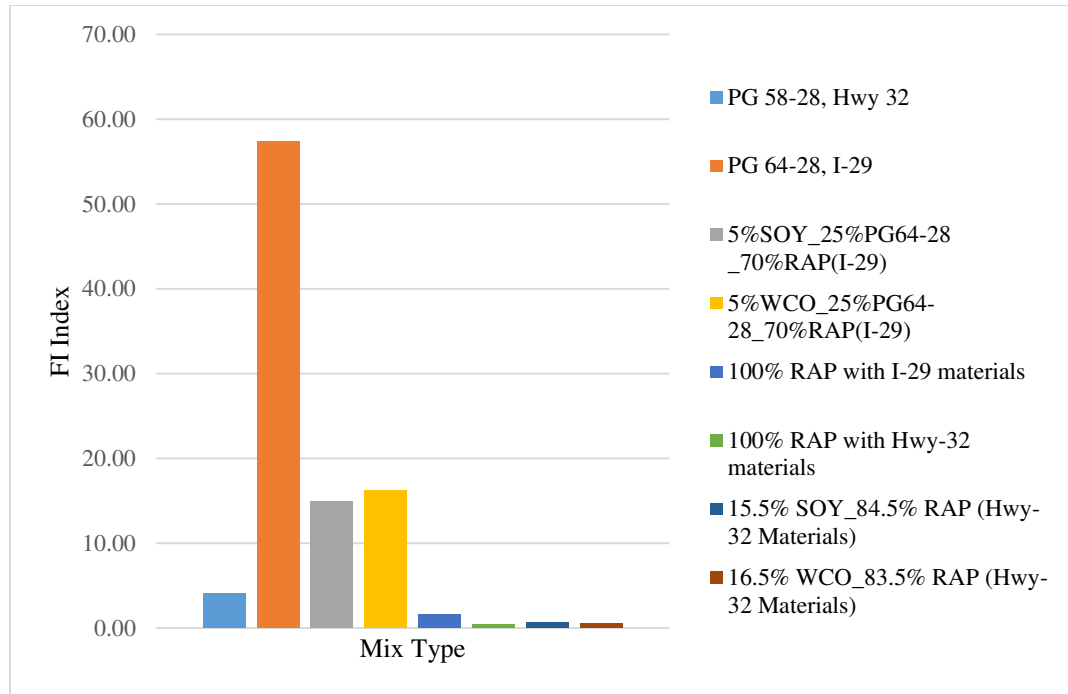


Figure 45: Average I-FIT index of different types of HMA mixes.

An independent t-test was performed on the different types of mixes to observe whether there was any significant difference or not between the mixture types. Summary of Independent t-test results is shown in Table 13. All the tests were done at 0.05 significance level. In the table, ‘N’ indicates that there is no significant difference between the mixes whereas ‘Y’ indicates that there is a significant difference between the mixes. From the results, it is observed that PG 58-28 mix and both 5%SOY\_25%PG64-28\_70%RAP and 5%WCO\_25%PG64-28\_70%RAP mixes did not show any significant difference. FI index also suggests the same. But the surprising result came out in the case of virgin mixtures of PG 58-28 and PG 64-28, which have shown the significant difference. Both 5%SOY\_25%PG64-28\_70% RAP mix and 5%WCO\_25%PG64-28\_70% RAP mixes did not show any significant difference with 100% RAP (I-29) mixes. However, FI index clearly showed that 100% RAP (I-29) is a poorly performing mixture compared to

good performing mixture of 5%SOY\_25%PG64-28\_70% RAP & 5%WCO\_25%PG 64-28\_70% RAP. These results are not conclusive because of small sample size.

Table 13: SCB Independent t-test Summary.

Mix type	Mix Type							
	PG 58-28, Hwy 32	PG 64-28, I-29	5%SOY_25%PG64-28_70%RAP(I-29)	5%WCO_25%PG64-28_70%RAP(I-29)	100% RAP (I-29)	100% RAP ( Hwy-32)	15.5% SOY_84.5% RAP (Hwy-32)	16.5% WCO_83.5% RAP (Hwy-32)
PG 58-28, Hwy 32	X	Y	N	N	Y	N	Y	Y
PG 64-28, I-29	X	X	Y	Y	Y	Y	Y	Y
5%SOY_25%PG64-28_70%RAP(I-29)	X	X	X	N	N	Y	Y	Y
5%WCO_25%PG64-28_70%RAP(I-29)	X	X	X	X	N	Y	Y	Y
100% RAP (I-29)	X	X	X	X	X	Y	Y	Y
100% RAP (Hwy-32)	X	X	X	X	X	X	N	N
15.5% SOY_84.5% RAP (Hwy-32)	X	X	X	X	X	X	X	N
16.5% WCO_83.5% RAP (Hwy-32)	X	X	X	X	X	X	X	X

#### 4.2.3 Low-Temperature Cracking Resistance

Resistance to low-temperature cracking of HMA mix specimen was analyzed by performing the DCT test. Both binders have the same low-temperature PG grade i.e. -28°C. That's why all the specimens were tested at -18°C as prescribed in ASTM D7313. As it was mentioned earlier that limited availability of aggregates and extracted RAP binder, all types of specimens couldn't be prepared and two specimens were prepared for each type of mixes. A higher fracture energy shows a good low-temperature cracking resistance. Average fracture energy and peak load obtained from the tests for different types of mixes is shown in Table 14. For 100% RAP binder with the Highway-32 aggregates, the specimens were very weak and failed during making hole in the specimen to meet the

geometric requirements, which is shown in Figure 46. A typical load-CMOD curve obtained from DCT test is shown in Figure 47. Average fracture energy for different mixes is shown in Figure 48. From the figure, it is observed that 5%WCO\_25%PG64-28\_70%RAP mixes show the highest average fracture energy among all the mixes including the virgin mixes. 5%SOY\_25%PG64-28\_70%RAP mixes show only 5% less energy than the PG64-28 mixes. 100% RAP mixes with the I-29 aggregates show the lowest fracture energy.

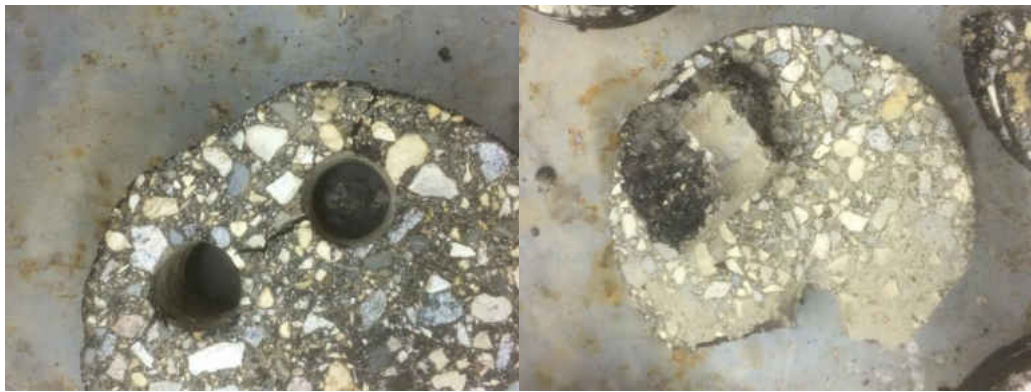


Figure 46: Images of failed 100% RAP DCT specimen during preparation.

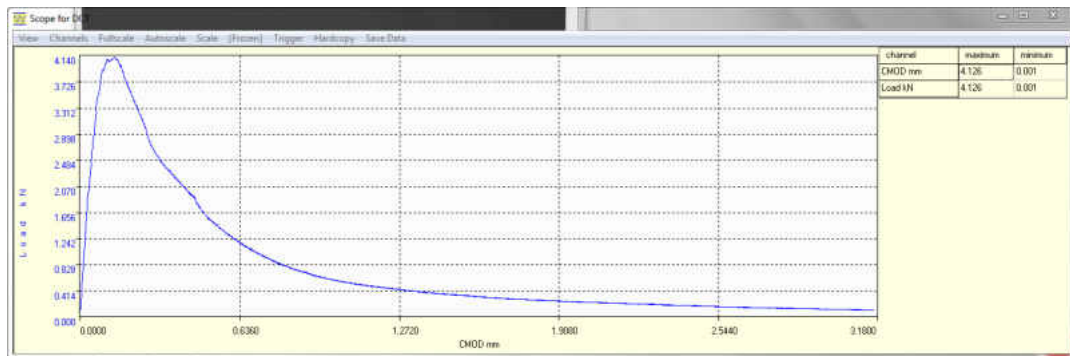


Figure 47: Typical Load vs CMOD curve obtained from DCT test.

Table 14: DCT Specimens Fracture Energies.

Sample Type	Average	
	Energy (J/m <sup>2</sup> )	Peak Load (kN)
PG 58-28 (Hwy 32 materials)	348.5	3.233

PG 64-28 (I-29 materials)	521.5	4.072
5%SOY_25%PG64-28_70%RAP (I-29 Materials)	498.5	4.0385
5%WCO_25%PG64-28_70%RAP (I-29 Materials)	563	3.9675
100% RAP (Hwy 32 materials)	Specimen failed during preparation	
100% RAP (I-29 materials)	21	2.976

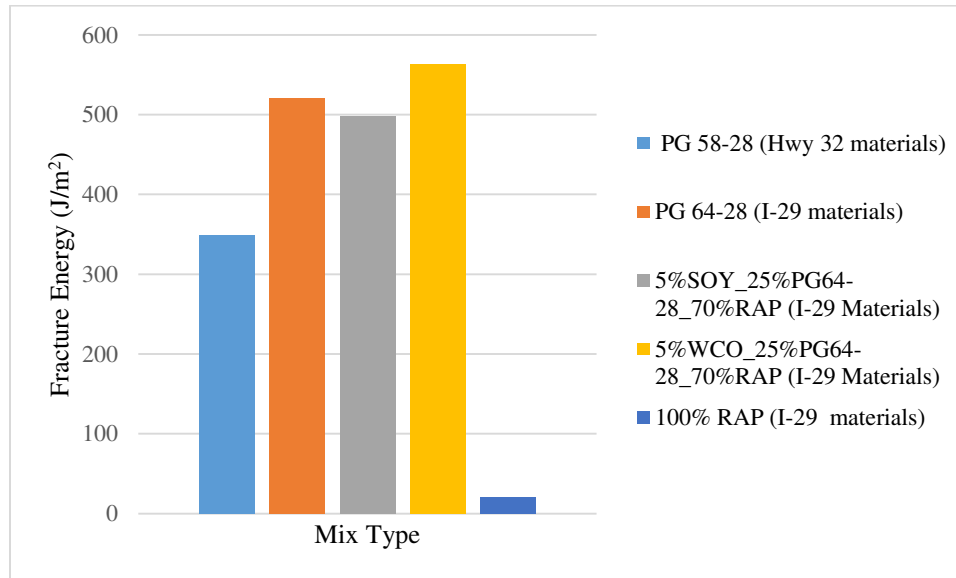


Figure 48: Average Fracture Energies for different types of mixtures.



## **CHAPTER V**

### **CONCLUSIONS AND RECOMMENDATIONS**

#### **5.0 General**

Increasing the percentage of RAP in HMA can lead to a path of sustainability. But a high percentage of RAP in HMA produces an overly stiff mix that is susceptible to fatigue and low-temperature cracking. The addition of bio-binder in the mix with high RAP has the potential to improve the fatigue and low-temperature cracking properties of HMA while maintaining an adequate rutting resistance. This research was done to assess the effects of bio-binder when it is used with a high percentage of RAP. Based on the analysis of the tests results, it was observed that modification of high RAP binder with bio-binder along with a certain percentage of virgin binder improves the fatigue and low-temperature cracking properties. Though the use of modified binder reduces the rutting resistance of the mix, rutting resistance is well below the set rut depth criteria.

#### **5.1 Rutting Resistance**

100% RAP binder performs better against rutting at high temperature. In the case of the unaged binder, all the modified binders couldn't pass the critical value of stiffness requirement except the virgin binder of PG58-28 and PG64-28. But when these binders were tested after RTFO aging, all the binders including the virgin binders passed the critical value of stiffness requirement except the 15.5%SOY\_84.5%RAP binder. In addition to that, 5%WCO\_25%PG64-28\_70%RAP binder produced almost the same results as PG64-

28 binder when tested at 64°C and 16.5%WCO\_83.5%RAP binder produced an almost the same result of the PG 58-28 binder when tested at 58°C.

From APA test, it was observed that all the specimens passed the rut depth criteria set in this study. 100% RAP binder showed the highest rutting resistance among the mixes. 5%SOY\_25%PG64-28\_70%RAP HMA mixes performed better than the PG64-28 and 5%WCO\_25%PG64-28\_70%RAP HMA mixes against rutting.

## **5.2 Fatigue Resistance**

The PAV aged modified binders by bio-binder with/without virgin binder were higher stiffness than the stiffness of both virgin binders. Stiffness of 5%SOY\_25%PG58-28\_70%RAP, 5%WCO\_25%PG58-28\_70%RAP, 15.5%SOY\_84.5%RAP, and 16.5%WCO\_83.5%RAP differ more with PG58-28 binder when these binders were tested at 58°C. But when the binders of 5%SOY\_25%PG64-28\_70%RAP and 5%WCO\_25%PG64-28\_70%RAP were tested at 64°C, the stiffness of virgin binder of PG64-28 didn't differ much and at 100% shear strain level stiffness of the modified binders was almost the same as the stiffness of virgin binder.

Though the 15.5%SOY\_84.5%RAP and 16.5%WCO\_83.5%RAP binders produced a good result in rheology test, both the mixes performed poorly against fatigue cracking in terms of fracture energy and FI index. Mixes with a virgin binder of PG64-28 performed best against fatigue cracking. 5%WCO\_25%PG64-28\_70%RAP HMA mix performed better than the 5%SOY\_25%PG64-28\_70%RAP HMA mix. 100% RAP HMA mix showed the lowest resistance against fatigue cracking as expected.

### **5.3 Low-Temperature Cracking Resistance**

The addition of bio-binder in high RAP binder with virgin binder produced better results against low-temperature cracking. Based on the low-temperature rheology test, 5%SOY\_25%PG64-28\_70%RAP and 5%WCO\_25%PG64-28\_70%RAP binder showed lower creep stiffness and higher slope ( $m_r$ ) in the master curve than the stiffness and slope of the master curve of the virgin binder. 100% RAP binder performed the worst among the binders. 5%SOY\_25%PG58-28\_70%RAP, 5%WCO\_25%PG58-28\_70%RAP produced similar results to virgin binder.

DCT test results also validated the low-temperature rheology test findings. 5%WCO\_25%PG64-28\_70%RAP HMA mix produced the highest fracture energy which means it possesses the highest low-temperature cracking resistance. 5%SOY\_25%PG64-28\_70%RAP mixes produced only 5% lower fracture energy than the fracture energy of PG64-28 mixes. 100% RAP mixes were the worst.

### **5.4 Limitations**

There were few limitations in the research which may have been reflected in the results. All types of HMA specimens based on binder combinations couldn't be prepared due to the aggregates and extracted RAP binder constraint. Besides, the number of specimens for all types of test were limited. Hence, an independent statistical significance test couldn't run for all types of tests. The thickness of SCB specimen was 25mm instead of 50mm recommended by I-FIT due to the insufficiency of materials.

### **5.5 Future Works**

Further works are needed to be done for assessing the effects of bio-binder on binder and HMA mix with a high percentage of RAP. The sample size for each test of

HMA specimen should be increased to get statistically significant results. Moreover, HMA specimen including all types of binder type should be prepared and tested to see the bio-binder effects on HMA specimen. The selections of a combination of binders in this research were based on maximizing the amount of RAP binder. Few other combinations of the binder may be tested to see the difference in the HMA properties. In the case of SCB test, specimen thickness can be made 50mm as it is the recommended thickness of the specimen. Overall, a better scenario of the effect of bio-binder on the HMA mix can be achieved by a field test.

## REFERENCES

- AASHTO. (2016). *Determining the Fracture Potential of Asphalt Mixtures Using Semicircular Bend Geometry (SCB) at Intermediate Temperature*. AASHTO.
- Abson, G., & Burton, C. (1960). *The Use of Chlorinated Solvents in the Abson Recovery Method*. St. Paul, MN: Association of Asphalt Paving Technologist.
- Al-Qadi, I. L., Carpenter, S. H., Roberts, G. L., Ozer, H., & Aurangzeb, Q. (2009). *Investigation of working binder in hot-mix asphalt containing recycled asphalt pavements*. Washington, D.C.: In 88th Annual Meeting of the Transportation Research Board.
- Al-Qadi, I. L., Carpenter, S. H., Roberts, G. L., Ozer, H., Aurangzeb, Q., Elseifi, M. A., & Trepanier, J. (2009). *Determination of Usable Residual Asphalt Binder in RAP*. Urbana, Illinois: Illinois Center for Transportation.
- Alsi, H., Ahmadinia, E., Zargar, M., & Karim, M. R. (2012). Investigation on physical properties of waste cooking oil- Rejuvenated bitumen binder. *Construction and Building Materials*, 398-405.
- ASTM. (2003). *Standard Test Method for Recovery of Asphalt From Solution by Abson Method*. West Conshohocken, PA: ASTM International.
- ASTM. (2004). *Standard Test Method for Effect of Heat and Air on a Moving Film of Asphalt (Rolling Thin-Film Oven Test)*. West Conshohocken, PA: ASTM International.
- ASTM. (2008). *Standard Test Method for Determining the Rheological Properties of Asphalt Binder Using a Dynamic Shear Rheometer*. West Conshohocken, PA: ASTM International.
- ASTM. (2011). *Standard Test Methods for Quantitative Extraction of Bitumen From Bituminous Paving Mixtures*. West Conshohocken, PA: ASTM International.
- ASTM. (2013). *Standard Test Method for Determining Fracture Energy of Asphalt-Aggregate Mixtures Using the Disk-Shaped Compact Tension Geometry*. ASTM International.

- ASTM. (2015). *Standard Test Method for Preparation and Determination of the Relative Density of Asphalt Mix Specimens by Means of the Superpave Gyrotory Compactor*. West Conshohocken, PA: ASTM International.
- ASTM. (2016). *Standard Test Method for Evaluation of Asphalt Mixture Cracking Resistance using the Semi-Circular Bend Test (SCB) at Intermediate Temperatures*. ASTM International.
- Bazant, Z. P., & Planas, J. (1997). *Fracture and size effect in concrete and other quasibrittle materials*. Boca: CRC Press.
- Brown, R. E., Kandhal, S. P., & Zhang, J. (2001). *Performance Testing for Hot Mix Asphalt*. National Center for Asphalt Technology, Report 01-05.
- Brundtland Commission. (1987). *Report of the World Commission on Environment and Development*. United Nations.
- Bukowski, J. R. (1997). *Guidelines for the Design of Superpave Mixtures Containing Reclaimed Asphalt Pavement (RAP)*. San Antonio, TX: FHWA Superpave Mixtures Expert Task Group.
- Burr, B. L., Davidson, R. R., Jemison, H. B., Glover, C. J., & Bullin, J. A. (1991). Asphalt Hardening in Extraction Solvents. *Journal of the Transportation Research Board*, 70-76.
- Chesner, W. H., Collins, R. J., & MacKay, M. H. (1998). *User guidelines for waste and by-product materials in pavement construction*. Federal Highway Administration (FHWA-RD-97-148).
- Chiangmai, C. N. (2010). *Fatigue-fracture relation on asphalt concrete mixtures*. Urbana-Champaign: Doctoral dissertation, University of Illinois at Urbana-Champaign.
- Choubane, B., Page, G., & Musselman, J. (2000). Suitability of Asphalt Pavement Analyzer for Predicting Pavement Rutting. *Journal of the Transportation Research Board*, 107-115.
- Christensen, R. (2012). *Theory of viscoelasticity: an introduction*. Elsevier.
- Colbert, B., & You, Z. (2012). The determination of mechanical performance of laboratory produced hot mix asphalt mixtures using controlled RAP and virgin aggregate size fractions. *Construction and Building Materials*, 26(1), 655-662.
- Collins-Garcia, H., Tia, M., Roque, R., & Choubane, B. (2000). Alternative Solvent for Reducing Health and Environmental Hazards in Extracting Asphalt: An Evaluation. *Journal of the Transportation Research Board*, 79-85.

- Copeland, A. (2011). *Reclaimed Asphalt Pavement in Asphalt Mixtures: State of the Practice*. McLean, VA: Federal Highway Administration.
- Enviro Tech International, Inc. (2008). *Ensolv Technical Data Sheet, Document No. 6000*.
- EPA. (2017, March 14). *EPA, United States Environmental Protection Agency*. Retrieved from <https://www3.epa.gov/region9/waste/>
- Farrar, M., Sui, C., Salmans, S., & Qin, Q. (2015). *Determining the Low-Temperature Rheological Properties of Asphalt Binder Using a Dynamic Shear Rheometer (DSR)*. Laramie, WY: Western Research Institute.
- FHWA. (2017, March 14). *Moving Ahead for Progress in the 21st Century (MAP-21)*. Retrieved from US Department of Transportation, Federal Highway Administration: <https://www.fhwa.dot.gov/map21/>
- Hansen, K. R., & Copeland, A. (2015). *Asphalt Pavement Industry Survey on Recycled Materials and Warm-Mix Asphalt Usage:2014*. Lanham: National Asphalt Pavement Association.
- Hill, B., Oldham, D., Behnia, B., Fini, E. H., Buttlar, W. G., & Reis, H. (2013). Low-Temperature Performance Characterization of Biomodified Asphalt Mixtures That Contain Reclaimed Asphalt Pavement. *Journal of the Transportation Research Board, 2371*, 49-57.
- Hill, B., Oldham, D., Behnia, B., Fini, E., Buttlar, W., & Reis, H. (2014). Low-Temperature Performance Characterization of Biomodified Asphalt Mixtures That Contain Reclaimed Asphalt Pavement. *Journal of the Transportation Research Board, 49-57*.
- Jacobs, M. M., Hopman, P. C., & Molenaar, A. A. (1996). Application of fracture mechanics principles to analyze cracking in asphalt concrete (with discussion). *Journal of the Association of Asphalt Paving Technologists, 1-39*.
- Kennedy, T. W., Tam, W. O., & Solaimanian, M. (1998). Optimizing use of reclaimed asphalt pavement with the Superpave system. *Journal of the Association of Asphalt Paving Technologists, 67*, 311-333.
- Khedr, S. A., & Breakah, T. (2011). Rutting parameters for asphalt concrete for different aggregate structures. *International Journal of Pavement Engineering, 13-23*.
- Kim, K. W., & El Hussein, H. M. (1995). Effect of differential thermal contraction on fracture toughness of asphalt materials at low temperatures (with discussion). *Journal of the Association of Asphalt Paving Technologists, 474-499*.

- Lee, N., Chou, C.-P., & Chen, K.-Y. (2012). *Benefits in Energy Savings and CO2 Reduction by Using Reclaimed Asphalt Pavement*. Washington, DC: Transportation Research Board 91st Annual Meeting.
- Lu, X., & Isacsson, U. (1998). Chemical and rheological evaluation of ageing properties of SBS polymer modified bitumens. *ELSEVIER*, 77(9-10), 961-972.
- Marasteanu, M., Zofka, A., Turos, M., Li, X., Velasquez, R., Li, X., . . . McGraw, J. (2007). *Investigation of Low Temperature Cracking in Asphalt Pavements National Pooled Fund Study 776*. Minnesota Department of Transportation.
- McDaniel, R. S., Huber, G. A., & Gallivan, V. (2006). Conserving Resources and Quality with High RAP Content Mixes. *HMAT: Hot Mix Asphalt Technology*, 44-46.
- McDaniel, R. S., Soleymani, H., Anderson, R. M., Turner, P., & Peterson, R. (2000). *Recommended Use of Reclaimed Asphalt Pavement in the SuperPave Mixture Design Method*. Washington, D.C.: NCHRP Final Report (9-12), Transportation Research Board.
- McDaniel, R., & Anderson, R. M. (2001). *Recommended Use of Reclaimed Asphalt Pavement in the SuperPave Mix Design Method: Technician Manual*. Washington, D.C.: NCHRP Report 452, Transportation Research Board.
- McDaniel, R., Shah, A., Huber, G., & Gallivan, V. (2007). Investigation of properties of plant-produced RAP mixtures. *Journal of the Transportation Research Board*, 103-111.
- McGraw, J., Iverson, D., Schmidt, G., & Olson, J. (2001). *Selection of an Alternative Asphalt Extraction Solvent*. St. Paul, Minnesota: Minnesota Department of Transportation.
- Mogawer, W. S., Fini, E. H., Austerman, A. J., Booshehrian, A., & Zada, B. (2016). Performance characteristics of high reclaimed asphalt pavement containing bio-modifier. *Road Materials And Pavement design*, 17(3), 753-767.
- Mogawer, W., Bennert, T., Daniel, J. S., Bonaquist, R., Austerman, A., & Booshehrian, A. (2012). Performance characteristics of plant produced high RAP mixtures. *Road Materials and Pavement Design*, 13, 183-208.
- NAPA. (2016). *National Asphalt Pavement Association Engineering*. Retrieved November 16, 2016, from <http://www.asphaltpavement.org>
- Ozer, H., Al-Qadi, I. L., Lambros, J., El-Khatib, A., Singhvi, P., & Doll, B. (2016). Development of the fracture-based flexibility index for asphalt concrete cracking



potential using modified semi-circle bending test parameters. *Construction and Building Materials*, 390-401.

Pavement Interactive. (2016, June 3). *Dynamic Shear Rheometer*. Retrieved from Pavement Interactive: <http://www.pavementinteractive.org>

Pavement Interactive. (2017, March 19). *Pavement Interactive*. Retrieved from <http://www.pavementinteractive.org/rutting/>

Read, J., & Whiteoak, D. (2003). *The Shell Bitumen Handbook, Fifth Edition*. ICE Publishing.

Roberts, F., Kandhal, P., Brown, E. R., Lee, D. Y., & Kennedy, T. (1996). *Hot Mix Asphalt Materials, Mixture Design and Construction* (2nd ed.). Lanham, MD: NAPA.

Sargand, S. M., & Kim, S. S. (2003). *Performance evaluation of polymer modified Superpave mixes using laboratory tests and accelerated pavement load facility*. Washington, D.C.: In 82nd Transportation Research Board Annual Meeting.

Seidel, J. C., & Haddock, J. E. (2012). *Soy fatty acids as sustainable modifier for asphalt binders*. Washington, D.C.: Transportation Research Board E-Circular.

Shen, J., Amirkhanian, S., & Miller, J. A. (2007). Effects of Rejuvenating Agents on Superpave Mixtures Containing Reclaimed Asphalt Pavement. *Journal of Material in Civil Engineering*, 376-384.

Skok, E., Johnson, E., & Turk, A. (2002). *Asphalt Pavement Analyzer (APA) Evaluation*. St. Paul, Minnesota: Minnesota Department of Transportation.

Stelljes, M. (2001). *Human in Vitro Bioassays of Solvents*. Clean Tech.

Sui, C., Farrar, M. J., Harnsberger, P. M., Tuminello, W. H., & Turner, T. F. (2011). *A new low-temperature performance grading method using 4mm parallel-plates on a DSR*. Washington, D.C.: Transportation Research Board 91st Annual Meeting Compendium of Papers.

Suleiman, N. (2008). *Evaluation of North Dakota's Aggregate Characteristics and Performance in Locally Produced HMA Mixtures Using the Asphalt Pavement Analyzer*. Bismarck, ND: North Dakota Department of Transportation.

Suleiman, N., & Mandal, S. (2013). *Evaluating the Rut Resistance Performance of Warm Mix Asphalts in North Dakota*. Washington, D.C.: Transportation Research Board 92nd Annual Meeting.

- Tran, N. H., Taylor, A., & Willis, R. (2012). *Effect of rejuvenator on performance properties of HMA mixtures with high RAP and RAS contents*. Auburn, Alabama: National Center for Asphalt Technology.
- Tyrion, F. C. (2000). Asphalt Oxidation: Asphaltenes and Asphalts. *Development of Petroleum Science, 40B*, 445-474.
- Valdes, G., Perez-Jimenez, F., Miro, R., Martinez, A., & Botella, R. (2011). Experimental study of recycled asphalt mixtures with high percentages of reclaimed asphalt pavement (RAP). *Construction and Building Materials, 1289-1297*.
- Van Winkle, C. I. (2014). *Laboratory and field evaluation of hot mix asphalt with high contents of reclaimed asphalt pavement*. University of Iowa.
- Wagoner, M. P., Buttlar, W. G., & Paulino, G. H. (2005). Disk-shaped compact tension test for asphalt concrete fracture. *Experimental Mechanics, 270-277*.
- Wang, H., You, Z., Goh, S. W., Hao, P., & Huang, X. (2011). *Evaluation on the High Temperature Rheological Properties of Rubber Asphalt by Dynamic Shear Rheometer Test and the Master Curve*. Washington, D.C.: Transportation Research Board 91st Annual Meeting Compendium of Papers.
- Wen, H., Bhusal, S., & Wen, B. (2013). Laboratory Evaluation of Waste Cooking Oil-Based Bioasphalt as an Alternative Binder for Hot Mix Asphalt. *Journal of Materials in Civil Engineering, 25(10)*.
- West, R., Kvasnak, A., Tran, N., Powell, B., & Turner, P. (2009). Testing of moderate and high reclaimed asphalt pavement content mixes: laboratory and accelerated field performance testing at the national center for asphalt technology test track. *Journal of the Transportation Research Record, 100-108*.
- Yang, X., You, Z., Dai, Q., & Mills-Beale, J. (2014). Mechanical performance of asphalt mixtures modified by bio-oils derived from waste wood resources. *Construction and Building Materials, 424-431*.

## APPENDICES

### HOT MIX DESIGN DATA-SUPERPAVE

Department of Transportation, Materials and Research (Rev. 3-16)

6/1/16

Mix Design Company:	Knife River Materials		
Lab No.			
Location	Adams to Edinberg	Project Specification	Section 430
Project	H-6-032(057)191 PCN-21538	Type of AC(top lift)	58-28
	SS-6-017(042)096 PCN-21276		
District	Grand Forks	Type of AC(bot lift)	58-28
County	Walsh	Letting Date	5/13/16
Date	6/1/16	Plus#4 (%)	41.0
Pit Owner(s)	KRM, Grabriel Const	Minus #4 (%)	59.0
Pit#1 Location	Pioneer (Fordville)		
Pit#2 Location	Gabriel	Gyratory Compactive Effort	
Pit#3 Location		Ninitial	7
		Ndesign	75
		Nmaximum	115

#### Mix Properties at Recommended Asphalt Content

	Mix Design	Specification
Optimum AC (%)	6.1	
Density(pcf)	143.7	
Air Voids (%)	4.0	2.0-6.0
VMA (%)	14.2	14.0 min
VFA (%)	71.6	65-78
%Gmm@Ninitial	87.4	89%max
%Gmm@Nmaximum	96.9	98%max
AC Film Thickness (m)	10.0	7.5-13.0
Dust/Effective AC Ratio	10.0	7.5-13.0
Fine Agg Angularity (%)	43.8	43min
Sand Equivalent (%)	49.5	40min
Coarse Agg Angularity (%)	87.0	75min
Flat/Elongated Pieces (%)	0.0	10max
Maximum SpG @ Ndes	2.399	

#### Summary of Aggregate

##### Characteristics from Mix Design

Gradation (%Passing)	Blend	Virgin
5/8"	100	100
1/2"	96.6	97.3
3/8"	85.5	86.9
#4	59.0	58.2
#8	40.7	39.9
#16	27.5	26.7
#30	16.3	15.4
#50	8.7	7.9
#100	6.0	5.5
#200	4.7	4.2
Virgin Add AC (%)		4.6
Virgin Agg. FAA (%)		43.5
Asphalt Absorption (%)		1.64
Water Absorption (%)		2.06
Light Wt Particles (%)		4.8
Toughness (% Loss)		NA
Specific Gravity Information		
Combined Bulk (Gsb)		2.520
-No. 4 Combined Bulk (Gsb)		2.470
-No. 4 Virgin Bulk (Gsb)		2.431
Apparent (Gsa)		2.720
Effective (Gme)		2.625

Remarks:

Mix Design Technician & ID: Danny Schmidt 1366

Distribution:  
Materials and Research, Grand Forks

Figure 49: PG58-28 HMA Mix Design Summary.

# HOT MIX DESIGN DATA-SUPERPAVE

Department of Transportation, Materials and Research (Rev. 3-16)

6/8/16

Mix Design Company:	Knife River Materials		
Lab No.			
Location	I-29 near St Thomas, Bowesmont	Project Specification	Section 430
Project	SIM-6-029(128)183 PCN-20796	Type of AC(top lift)	64-28
	NH-6-081(089)204 PCN-21130		
District	Grand Forks	Type of AC(bot lift)	58-28
County	Pembina, Walsh	Letting Date	12/16/15
Date	6/8/16	Plus#4 (%)	33.8
Pit Owner(s)	Thygeson	Minus #4 (%)	66.2
Pit#1 Location	Deerwood township, Kittson co MN		
Pit#2 Location		Gyratory Compactive Effort	
Pit#3 Location		Ninitial	7
		Ndesign	75
		Nmaximum	115

### Mix Properties at Recommended Asphalt Content

	Mix Design	Specification
Optimum AC (%)	5.4	
Density(pcf)	149.1	
Air Voids (%)	4.0	2.0-6.0
VMA (%)	14.1	14.0 min
VFA (%)	71.7	65-78
%Gmm@Ninitial	87.0	89%max
%Gmm@Nmaximum	97.5	98%max
AC Film Thickness (m)	9.5	7.5-13.0
Dust/Effective AC Ratio	0.9	0.6-1.3
Fine Agg Angularity (%)	45.5	45min
Sand Equivalent (%)	71.3	40min
Coarse Agg Angularity (%)	88.0	85min
Flat/Elongated Pieces (%)	0.0	10max
Maximum SpG @ Ndes	2.489	

### Final Aggregate Blend (%)

9	N Fines	Deerwood
18	Rock	Deerwood
44	Washed Dust	Deerwood
9	Dust	Deerwood
20	RAP	

### Summary of Aggregate

#### Characteristics from Mix Design

Gradation (%Passing)	Blend	Virgin
5/8"	100	100
1/2"	99.6	100.0
3/8"	91.5	91.7
#4	66.2	64.2
#8	41.3	37.8
#16	28.1	25.1
#30	18.5	15.8
#50	12.0	10.5
#100	6.0	4.5
#200	4.1	2.9
Virgin Add AC (%)		4.1
Virgin Agg. FAA (%)		45.1
Asphalt Absorption (%)		1.02
Water Absorption (%)		1.08
Light Wt Particles (%)		0.0
Toughness (% Loss)		NA
Specific Gravity Information		
Combined Bulk (Gsb)		2.633
-No. 4 Combined Bulk (Gsb)		2.625
-No. 4 Virgin Bulk (Gsb)		2.618
Apparent (Gsa)		2.705
Effective (Gme)		2.703

### Remarks:

Also project SIM-6-029(110)183 PCN-18961

Mix Design Technician & ID: Danny Schmidt 1366

Distribution:  
Materials and Research, Grand Forks

Figure 50: PG64-28 HMA Mix Design Summary.